374 J. Med. Chem. 2010, 53, 374–391
DOI: 10.1021/jm901319p

Journal of Medicinal Chemistry Article

1,2,4-Triazolyl Azabicyclo[3.1.0]hexanes: A New Series of Potent and Selective Dopamine D_3 Receptor Antagonists

Fabrizio Micheli,*[,†,§] Luca Arista,[+] Giorgio Bonanomi,[†,§] Frank E. Blaney,[⊥,▽] Simone Braggio,[†,§] Anna Maria Capelli,[‡,§] Anna Checchia,[†,§] Federica Damiani,[^] Romano Di-Fabio,[†,§] Stefano Fontana,[†,§] Gabriella Gentile,[†,§] Cristiana Griffante,[†,§] Dieter Hamprecht,[¶] Carla Marchioro,[‡,§] Manolo Mugnaini,[†,§] Jacqui Piner,[#,▽] Emiliangelo Ratti,[∥,▽] Giovanna Tedesco,[‡,§] Luca Tarsi,[†,§] Silvia Terreni,[†,§] Angela Worby,[⊥,▽] Charles R. Ashby Jr.,[○] and Christian Heidbreder[◆]

[†]*Neurosciences Centre of Excellence,* [‡]*Molecular Discovery Research,* [§] *GlaxoSmithKline Medicines Research Centre, Via Fleming 4, 37135 Verona, Italy,* [∥] *Neurosciences Centre of Excellence,* [⊥]*Molecular Discovery Research,* [#]*Safety Assessment,* [▽]*GlaxoSmithKline Medicines Research Centre, NFSP, Harlow, U.K.,* [○]*Department of Pharmaceutical Sciences, Saint John's University, Jamaica, New York 11439,* [◆]*Reckitt Benckiser Pharmaceuticals, Richmond, Virginia 23235,* [¶]*Boehringer Ingelheim, Milan, Italy,* [+]*Novartis Institute Research, Basel, Switzerland, and* [^]*European Patent Office, Munich, Germany*

Received September 4, 2009

The discovery of new highly potent and selective dopamine (DA) D_3 receptor antagonists has recently allowed the characterization of the DA D_3 receptor in a range of preclinical animal models of drug addiction. A novel series of 1,2,4-triazol-3-yl-azabicyclo[3.1.0]hexanes, members of which showed a high affinity and selectivity for the DA D_3 receptor and excellent pharmacokinetic profiles, is reported here. Members of a group of derivatives from this series showed good oral bioavailability and brain penetration and very high in vitro affinity and selectivity for the DA D_3 receptor, as well as high in vitro potency for antagonism at this receptor. Several members of this series also significantly attenuate the expression of conditioned place preference (CPP) to nicotine and cocaine.

Introduction

The location of the dopamine (DA[a]) D_3 receptor in the rodent and human brain, changes in the expression of these receptors upon exposure to drugs of abuse, and a growing body of preclinical evidence in models of substance dependence, suggest that selective DA D_3 receptor antagonists may be a point of therapeutic intervention for substance dependence or abuse [for reviews see refs 1−6]. The observation that selective DA D_3 receptor antagonists regulate the motivation to self-administer drugs and disrupt drug-associated cue-induced craving has contributed in guiding state-of-the-art medicinal chemistry research efforts to develop a highly selective DA D_3 receptor antagonist.

We have recently reported[7] that a series of 1,2,4-triazol-3-yl-thiopropyl-tetrahydrobenzazepines, which have high in vitro and in vivo selectivity, can significantly attenuate or block the effects of drugs of abuse in a number of animal models of addiction. The aim of the present work is related to the pioneering and original substitution, for this specific thiotriazole series, of the benzoazepine (BAZ) scaffold by a aryl azabicyclo[3.1.0]hexane template that is endowed with promising developability characteristics; a detailed structure activity relationship (SAR) and a series of in vitro and in vivo experiments are provided to characterize this series of highly potent and selective DA D_3 receptor antagonists.

Chemistry

During the past decade, one aspect of GSK research in CNS drug discovery was directed toward the discovery of novel chemical entities (NCEs) that selectively modulate the DA D_3 receptor. The successful result of this work led to the discovery of *trans-N*-[4-[2-(6-cyano-1,2,3,4-tetrahydroisoquinolin-2yl)-ethyl]cyclo-hexyl]-4-quinolinecarboxamide (SB-277011, **1**)[5,6] and to the more recent BAZ scaffolds 7-(1,3-dimethyl-1*H*-pyrazol-5-yl)-3-(3-{[4-methyl-5-(2-methyl-5-quinolinyl)-4*H*-1,2,4-triazol-3-yl]thio}propyl)-2,3,4,5-tetrahydro-1*H*-3-benzazepine (**2**),[7] 2-methyl-7-(3-{[4-methyl-5-(2-methyl-5-quinolinyl)-4*H*-1,2,4-triazol-3-yl]thio}propyl)-6,7,8,9-tetrahydro-5*H*-[1,3]oxazolo[4,5-*h*][3]benzazepine (**3**),[8] and 8-(3-{[4-methyl-5-(2-methyl-5-quinolinyl)-4*H*-1,2,4-triazol-3-yl]thio}propyl)-2-(trifluoromethyl)-7,8,9,10-tetrahydro-6*H*-[1,3]oxazolo[4,5-*g*][3]benzazepine (**4**)[9] (Figure 1).

The major step forward from **1** to the last three BAZ derivatives (**2**−**4**) was the introduction into the scaffold of appropriate developability characteristics (i.e., acceptable P450 profile, low intrinsic clearance (Cl_i), and good bioavailability (F%)) in preclinical species. Furthermore, in contrast to other DA D_3 receptor antagonists,[5,6] derivative **2** showed a reduced hERG liability in vitro and no prolongation of the QTc interval in vivo.[7] Given these positive preclinical results, our next goal was to investigate the possibility to achieve a similar preclinical profile using a different template. Accordingly, we planned to

*To whom correspondence should be addressed. Phone: +39-045-8218515. Fax: +39-045-8218196. E-mail: Fabrizio.E.Micheli@gsk.com.

[a] Abbreviations: BAZ, benzoazepine; CPP, conditioned place preference; ACh, acetylcholine ; hERG, human ether-a go-go K^+ channel; NCE, novel chemical entity; PK, pharmacokinetic; P450, cytochrome P450; hCl_i, human intrinsic clearance; MW, molecular weight; clogD, calculated logD; PSA, polar surface area; F%, bioavailability; B/B, brain/blood; Cl_b, blood clearance; V_d, distribution volume; SDM, site-directed mutagenesis; FLIPR, fluorescent imaging plate reader; GPCR, G-protein coupled receptor; TM, trans membrane; SPA, scintillation proximity assay; ECG, electrocardiogram; DA, dopamine; NT, not tested.

 Published on Web 11/05/2009

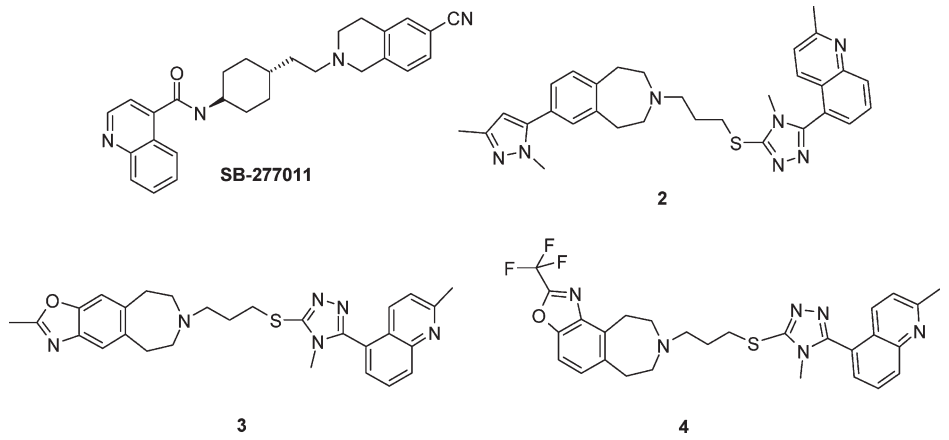

Figure 1. Structures of the previously reported GSK selective DA D_3 receptor antagonists.

Scheme 1. General Synthetic Procedures for the Preparation of Compounds **5**−**105**[a]

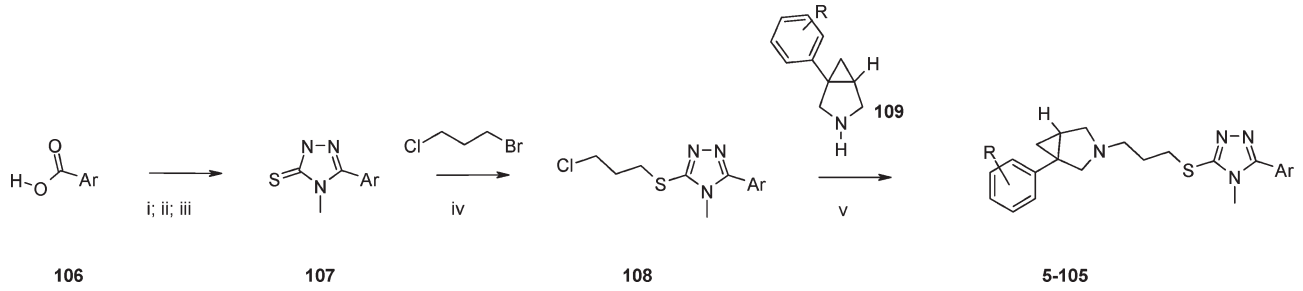

[a] (i) T3P in AcOEt; (ii) 4-methyl-3-thiosemicarbazide; (iii) NaOH; (iv) K_2CO_3/acetone; (v) K_2CO_3/DMF or CH_3CN.

explore if, in this specific series of aryl thiotriazoles, the BAZ scaffold could be replaced with an alternative basic moiety.

Results and Discussion

There are several options to approach the potential replacement of a certain portion of a molecule within a given scaffold: it is possible either to use a database of commercial or in house ring systems, to perform literature searches, to rely on de novo design, or to go through a massive combinatorial task replacing the given portion with all the fragments available in a specific store. For this specific thiotriazole system, a mix of all these techniques was used to replace the BAZ moiety, and a number of different structures were identified. Among them, the potential BAZ replacement that is reported in this manuscript is represented by an aryl azabicyclo[3.1.0]hexane moiety. The choice of this original scaffold was based on a number of reasons including the attractive physicochemical characteristics, predicted in silico (namely the polar surface area and the calculated logD) and, despite the associated structural complexity, the possibility to appropriately decorate the pendant aryl ring of the azabicyclo[3.1.0]hexane due to some in house synthetic experience.

By exploiting a screening cascade previously reported,[7] all the newly prepared compounds were assayed for their agonistic and antagonistic properties using a functional GTPγS assay expressing the human DA D_3 receptor. To proceed with this cascade, the NCEs had to fulfill the following key characteristics: (1) at least 100-fold selectivity vs DA D_2 and histamine H1 receptors (functional assays), and (2) 100-fold selectivity vs the hERG ion channel (dofetilide binding assay). Furthermore, to ensure that the selected templates were endowed with appropriate pharmacokinetic (PK) and developability characteristics from the beginning of the exploration, the NCEs went through generic developability screens such as CYPEX bactosome P450 inhibition and rat and human in vitro clearance in liver microsomes early in the screening cascade.

In contrast to the previously described BAZ system,[7] the aryl azabicyclo[3.1.0]hexane contains two stereogenic centers. Accordingly, both the racemate and each single enantiomer were submitted to test. Compounds were prepared according to Scheme 1. Additional information can also be found in refs 10,11.

The results of the exploration are reported in Tables 1−3.

The first compound of the series to be prepared and to be considered the reference point of our exploration was the racemic nonsubstituted phenyl azabicyclo[3.1.0]hexane **5** and its pure enantiomers **6** and **7**, respectively. This is usually an important step in generating SAR to fully appreciate the role of the substituents that will decorate a system, although the unsubstituted systems might sometime behave differently from the decorated ones. In this specific case, derivative **7** not only showed a similar potency at the DA D_3 receptor compared to derivative **1** but also had a 40-fold selectivity over the DA D_2 receptor. These results suggested that the working hypothesis might be correct and constituted a good starting point for further exploration. Interestingly enough, but not unexpectedly, a difference in affinity at the DA D_3 receptor was also noticed in the two enantiomers. The docking[7] of derivative **2** in the DA D_3 receptor model seemed to suggest the need for a lipophilic area in the region where the BAZ sits and the presence of some specific interactions with the hydrophilic pyrazole substituent (close to S182 and S192). For that reason, the meta/para position of the pendant aromatic ring on the azabicyclo[3.1.0]hexane was appropriately explored,

Table 1. Functional Activity at the Human DA D_3 Receptor and Selectivity for Quinolinyl Derivatives[a]

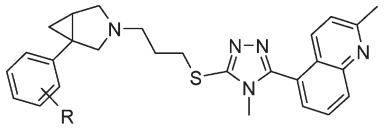

5-24

entry	R	hD_3-GTPγS fpK_i	hD_2-GTPγS fpK_i	hH_1-FLIPR pKb	hERG pIC_{50}	PSA[b]	cLogD[c]
1	not applicable	8.4	6.4	6.2	5.7	69	3.8
2	not applicable	8.8	6.5	6.1	5.7	65	5.3
3	not applicable	7.2	< 5.6	< 5.6	< 5.0	98	5.0
4	not applicable	8.4	< 6.1	6.3	5.7	73	6.3
5	H (rac)	7.6	6.8	7.3	5.7	47	3.4
6	H (se)	< 6.3	< 5.5	7.2	5.3	47	3.4
7	H (se)	8.3	6.7	NT	6.1	47	3.4
8	3,4-diCl (rac)	7.9	5.3	7.3	6.2	47	5.2
9	3,4-diCl (se)	7.4	6.4	7.2	5.8	47	5.2
10	3,4-diCl (se)	6.8	5.9	7.5	6.0	47	5.2
11	4-*t*-Bu (rac)	8.8	6.5	5.8	6.6	47	5.4
12	4-*t*-Bu (se)	7.7	5.7	NT	6.6	47	5.4
13	4-*t*-Bu (se)	8.7	6.1	NT	6.6	47	5.4
14	4-Br (rac)	8.4	5.4	7.7	6.9	47	4.5
15	4-Br (se)	< 6.3	< 6.1	7.0	6.3	47	4.5
16	4-Br (se)	8.9	< 6.1	6.6	6.6	47	4.5
17	4-CN (rac)	7.5	5.2	7.3	6.2	71	3.1
18	4-OMe (rac)	8.2	5.9	7.4	6.2	56	3.5
19	4-OMe (se)	8.9	< 6.4	7.5	6.2	56	3.5
20	4-OMe (se)	7.5	5.9	6.6	5.6	56	3.5
21	4-Cl (rac)	8.2	< 6.2	6.0	6.7	47	4.3
22	4-Cl (se)	9.0	6.7	6.3	5.8	47	4.3
23	4-Cl (se)	7.4	6.1	7.8	5.7	47	4.3
24	4-CF_3 (rac)	9.1	< 5.9	6.8	6.8	47	4.5

[a] fpK_i = functional pK_i obtained from the GTPγS functional assay. FLIPR = fluorescent imaging plate reader. SEM for D_3 GTPγS, H1 FLIPR, and HERG data sets is ±0.1 and for the D_2 GTPγS data is ±0.2. (rac) = racemate. (se) = single enantiomer. [b] Å^2. [c] ACD logD 7.4. version 11.

and the results are reported in Table 1. The 3,4-dichloro substitution (**8**−**10**) increased the lipophilicity to 5.2 without leading to an increased potency at the desired target, while the bulkier 4-*t*-butyl derivative (**11**−**13**, clogD = 5.4) increased the potency at D_3 and selectivity over the DA D_2 receptor (400-fold). This observation might result from the steric clash with some residues in the DA D_3 receptor of the substituents in position 3 and 4 of the aryl ring with respect to the single 4-substitution, even if the binding pocket in the receptor model appeared to be rather tolerant. A reduction of steric hindrance and clogD was achieved with the bromo derivatives (**14**−**16**, clogD = 4.5) and with the chloro derivatives (**21**−**23**, clogD = 4.3) without affecting significantly the affinity at the desired target. The introduction of the highly polar and hydrophilic cyano derivative **17** led to a reduction in affinity at the desired target with limited effect on hERG affinity. The electron-donating properties of the methoxy derivatives (**18**−**20**) did not seem to have a major influence on the affinity in this series. The highest potency and selectivity at the desired target (> 1000 fold over DA D_2 receptor and > 100 over H1 and hERG targets) were achieved with the p-CF_3 derivative **24**. This derivative was also endowed with a promising in vitro PK profile (inhibition on all P450 isoforms > 1 μM and relatively low hCl_i, namely 1.1 mL/min/g liver). In this specific series, the higher affinity achieved at the DA D_3 receptor was linked to one specific isomer, which was characterized as the enantiomer endowed with the (1*S*,5*R*) absolute stereochemistry. This attribution was achieved both through vibrational circular dichroism (VCD) and X-ray techniques; further and more specific details on this topic will be the subject of a separate analytical communication. Once completed, this first and very preliminary investigation of the left-hand side part of the molecule was followed by an introductory exploration of the right-hand side of the thiotriazole portion of the template. Considering the overall activity shown by the substituents reported in Table 1 on the aryl system, the trifluoromethyl group was kept as the reference point, and the single (1*S*,5*R*)-[3.1.0]hexane enantiomer was chosen for the exploration; nonetheless, to confirm the validity of the working hypothesis associated to the stereochemistry of the compound, one of the derivatives was prepared as a racemate; the single enantiomers were subsequently separated and were both independently evaluated for their biological activity. The results of this exploration are reported in Table 2. The regioisomeric quinoline **25** showed an increase in potency and a slightly reduced hERG activity; the introduction of more basic/hydrophilic substituents (**27**−**34**) led to a general slight reduction of activity both at the hERG and at the DA D_3 receptor, leading to a more balanced profile. Derivatives **27** and **28** showed low hERG affinity with a well-adjusted profile which included good in vitro PK properties (inhibition on all P450 isoforms was > 10 μM for both derivatives and their hCl_i was respectively 1.7 and 1.0 mL/min/g liver); therefore, both derivatives were further progressed to assess their in vivo PK properties in preclinical species.[12] After oral administration, they both showed moderate Cl_b in rats (18 and 13 mL/min/kg, respectively), identical half-life ($T_{1/2}$ = 2.1 h), similar distribution volumes (V_d = 2.5 and 2.2 L/kg, respectively), and almost identical bioavailability (F% = 50 and 46%, respectively); the brain penetration values were also comparable (B/B = 1.6 and 2, respectively), making them ideal candidates for further progression.

Table 2. Functional Activity at the Human DA D_3 Receptor and Selectivity for 4-Trifluoromethyl Derivatives[a]

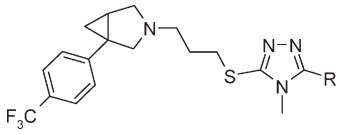

entry	R	hD_3-GTPγS fpK_i	hD_2-GTPγS fpK_i	hH_1-FLIPR pKb	hERG pIC_{50}	PSA[b]	cLogD[c]
25	2-methyl-6-quinolinyl (se)	9.6	6.2	7.3	6.3	47	4.5
26	phenyl (se)	9.2	6.8	7.4	6.2	34	4.1
27	2-methyl-3-pyridinyl (se)	9.0	6.5	6.9	5.3	47	3.1
28	4-pyridazinyl (se)	9.0	6.7	7.0	5.4	60	1.4
29	5-pyrimidinyl (se)	8.8	< 6.0	7.3	5.5	60	2.1
30	3-methyl-2-furanyl (se)	9.3	6.4	7.1	6.7	47	3.9
31	6-methyl-3-pyridinyl (se)	9.1	6.2	7.1	6.1	47	2.7
32	2,4-dimethyl-1,3-thiazol-5-yl (se)	9.6	6.6	7.4	5.7	47	2.1
33	5-methyl-2-pyrazinyl (se)	9.2	6.3	7.2	6.1	60	2.6
34	4-methyl-1,3-oxazol-5-yl (rac)	9.3	6.9	7.4	6.0	60	2.1
35	4-methyl-1,3-oxazol-5-yl (se)	9.0	7.0	7.5	6.1	60	2.1
36	4-methyl-1,3-oxazol-5-yl (se)	7.3	< 6.1	7.5	6.2	60	2.1

[a] fpK_i = functional pK_i obtained from the GTPγS functional assay. FLIPR = fluorescent imaging plate reader. SEM for D_3 GTPγS, H1 FLIPR, and HERG data sets is ±0.1 and for the D_2 GTPγS data is ±0.2. [b] Å^2. [c] ACD logD 7.4. version 11.

Derivatives **32** and **34** also showed excellent in vitro properties considering both their affinity/selectivity values and their PK profile; accordingly, they also underwent in vivo PK evaluation in rats. The thiazolyl derivative **32** showed an overall good PK profile after oral administration with a moderate Cl_b (26 mL/min/kg), a half-life value ($T_{1/2}$ = 2.0 h) comparable to that of previously analyzed derivatives, a moderate distribution volume (V_d = 3.9 L/kg), a moderate bioavailability (F% = 23%), and a good brain penetration (B/B = 2.2). The oxazolyl derivative **34** showed a low Cl_b (14 mL/min/kg), a comparable half-life ($T_{1/2}$ = 3.2 h), a similar distribution volume (V_d = 3.5 L/kg), and superior bioavailability and brain penetration (F% = 85% and B/B = 3.6, respectively).

The (1*S*,5*R*) derivative **35**, in agreement with the working plan, was the product endowed with the highest affinity at the DA D_3 receptor and was therefore further characterized as single enantiomer: its in vitro and in vivo PK profiles fully matched the results already observed with the racemic derivative **34**. Considering their general profile and the good selectivity window achieved, these results led to a further characterization of all these products in the screening cascade as described below.

At this point of the exploration, despite the identification of a number of potentially interesting compounds to be fully characterized along the screening cascade, a second SAR expansion of the left-hand side was carried out. In this further iteration, the newly identified heteroaromatic systems were maintained on the right-hand side of the molecule, whereas a computational strategy was applied as previously described.[7] It was noticed that, in the previous BAZ template, the key elements responsible for the activity of the molecule at the DA D_3 receptor were also responsible for the activity within the hERG channel. At that time, the visualization within the DA D_3 receptor model and within the hERG channel model of the amino acid residues interacting with specific regions of the molecule allowed the rational design of the best substituents able to maximize the window between these two affinities. Briefly, both the DA D_3 receptor (Figure 2A) and the hERG channel model[7] (Figure 2B) were used to dock the compounds and to assess the substituents that maintain the specific interactions in the DA D_3 model (namely the salt bridge between the basic nitrogen and Asp110 on transmembrane helix 3 (TM3), the interaction with Ser192 (TM5) and Ser182 (second extracellular loop), and the potential π-stacking interactions with Phe345 and His349 (TM6)). At the same time, those appropriately identified substituents should be able to disrupt the interactions of the molecule within the hERG channel (namely the specific interactions with Tyr652 and Phe656 in the S6 helices and the ones in the pore turn region of the channel model), particularly by reducing their aromatic π interactions.

It is worth noting that the DA D_3 receptor model can explain the DA D_3/D_2 selectivity of these compounds because of the hydrogen bond between the triazole ring and Thr368. The corresponding residue in the DA D_2 receptor is a phenylalanine (Phe), which would be expected to cause a severe steric clash with these ligands.

In the current exploration, in addition to the decorations of the aryl group identified from the modeling work mentioned above, a further selection of substituents with different physicochemical properties was also included to probe the SAR for this series.

Among the different right-hand side heteroaromatic derivatives reported in Table 2 and used in this exploration, we would like to report here the results achieved with the oxazolyl moiety present in derivative **35**. These results are tabulated in Table 3. The derivatives were synthesized and tested both as racemates and single enantiomers to verify if the "favorite" stereochemistry previously identified to achieve the higher affinity on the DA D_3 receptor (i.e., the (1*S*,5*R*) stereochemistry) was specific only for that thiotriazole subseries series or might have had a wider application in this specific series of aryl [3.1.0] thiotriazoles.

Once again, it was decided to start the exploration using the unsubstituted phenyl derivative **37** as reference compound, and in agreement with the need of SAR generation, some of the previously used substituents were also analyzed. In this specific subseries, in agreement with what is reported in Table 1, no major variation in the DA D_3 affinity was noticed among the 4-*t*-Bu (**40**), the 4-Br (**42**), and the 4-Cl (**51**) substituents; the major difference was linked to lipophilicity values and to the selectivity versus the H1 and DA D_2 receptors of compound **51**. A further reduction in the size of

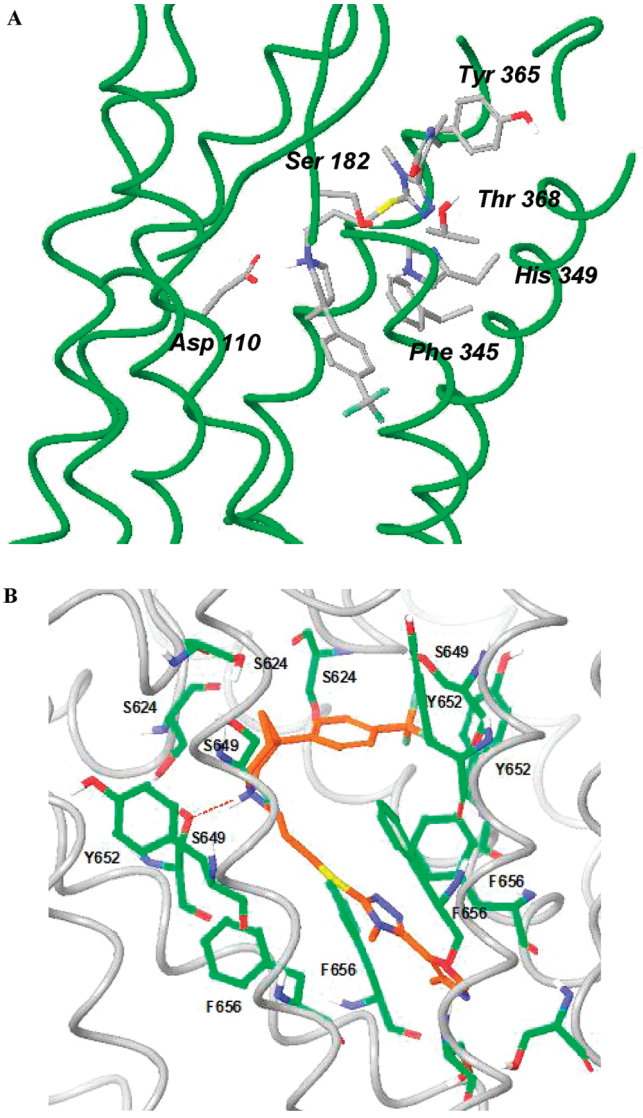

Figure 2. (A) Relevant interactions of derivative **35** in docking to the DA D_3 receptor model. Portions of the backbone ribbon has been removed for clarity. (B) Interactions of compound **35** in the hERG channel models. The backbone ribbon of the pore domain is included but that of the S5 and S6 helices has been removed for clarity. For details about the modeling techniques, please refer to ref 7.

the substituent in position 4 (F, **57**) led to a reduced affinity at the primary target. The slight reduction of DA D_3 affinity observed with the 4-OMe derivative **45** might be associated with its electrodonating properties, as the same effect was not observed with the 4-OCF_3 derivative **67**. The single substitution in position 3 of the aryl ring also seems to parallel the results already achieved in the subseries reported in Table 1, with the exception of the 3-CF_3 derivative **63**, where an increase in the affinity at the primary target led also to a slight increase in the affinity at the DA D_2 receptor. The next step in the analysis of the results of the exploration is related to the double substitution of the phenyl system. This was done using substituents that did not raise the clogD values to unacceptably high values. The 3,4-bis-chloro substitution in derivative **70**, in this specific subseries, did not suffer of the slight decrease in affinity at the primary target previously reported for the quinoline derivative **8**; unfortunately, this substitution did not achieve the desired selectivity over the DA D_2 receptor. The 2-F, 4-CF_3 derivative **74** showed an overall very balanced profile, while the 2-F, 4-Me derivative **93** exhibited a reduced affinity at the desired receptor; this might be related to its lower lipophilicity as potentially confirmed by the results of the 2F, 4-Cl derivative **96**. The 4-F, 3-CF_3 substitution (**77**) led to the highest DA D_3 affinity observed in this subseries, possibly due to the substituent in position 3 potentially interacting at best with the appropriate residues within the receptor pocket, as also observed for derivative **63**. Again, the introduction of potentially electrodonating properties in the methoxy derivative **99** led to a slight decrease in affinity in agreement with what was observed for derivative **44**. A simultaneous substitution of both "meta" positions, as in the 3,5- substituted derivative **89**, showed positive results as far as the affinity at the primary target was concerned, but the selectivity at the DA D_2 receptor was slightly reduced.

Among the compounds that were selected in agreement with the receptor/channel models studies for their electron-withdrawing ability and, therefore, for their potential ability to negatively affect the π interactions within the hERG channel, derivatives **51**, **74**, **77**, **84**, and **86** showed an overall balanced affinity profile; from the in vitro PK point of view, they showed the appropriate P450 and Cl_i parameters to be further progressed in vivo and accordingly they were chosen for further characterization. The best in vivo profiles obtained after oral administration in rats were associated with derivatives **51** and **74** that showed a moderate Cl_b (40 and 18 mL/min/kg, respectively), a sufficiently long half-life ($T_{1/2}$ = 1.3 and 3.7 h), a moderate distribution volume (V_d = 2.6 and 4.3 L/kg) associated with a good bioavailability (F% = 31% and 47%), and brain penetration (B/B = 2.7 and 3.1, respectively). Therefore, in addition to the compounds previously identified, these two derivatives were also selected for further characterization.

To ensure that no potential gaps were left during the chemical exploration of this new template, an automated analysis of all the DA D_3 fpK_i and hERG pIC_{50} data was performed using the SAR-Toolkit[13] in addition to the "classical" computational techniques described so far.

The "R-group/D-score" analysis is available as part of the SAR-Toolkit, a GSK proprietary suite of applications for SAR data analysis, based on the Daylight Toolkit[14] and embedded within Spotfire DecisionSite.[15] A highly versatile fragmentation tool defines the core portion of the molecules and the specific substituents (R-groups) within the set of molecules of interest (e.g., RG-Core, RG-R1, and RG-R2). Pairs of compounds which differ only in one R-group are then automatically identified, and the activity of the compound with an R-group chosen as reference is compared with that of a molecule carrying a replacement R-group. To assess whether the change is beneficial or detrimental for activity, a D-score is calculated as the average difference in activity across all the pairs of compounds carrying respectively the R-group of interest and the reference R-group and differing only by that R-group. All the compounds reported here constituted the original data set. Compound **37** in Table 3 was used as a reference structure. Using the right-hand side of the molecule as core structure and making use of the pendant substituents on the [3.1.0] scaffold as RG-R2, it appears quite clear from Figure 3 that in this specific subseries more lipophilic substituents seem to boost the DA D_3 activity. It is interesting to note that bulky substituents in the ortho position of the aromatic system (e.g., $-CF_3$ **65**, $-CH_3$ **75**) were less tolerated in this specific subseries. This is probably due to a conformational effect as the o-F derivative **74** (the fluorine atom being slightly

Table 3. Functional Activity at the Human DA D_3 Receptor and Selectivity for 5-Oxazolyl Derivatives[a]

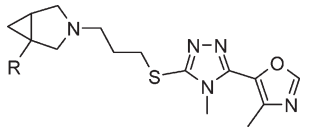

entry	R	hD_3-GTPγS fpK_i	hD_2-GTPγS fpK_i	hH_1-FLIPR pKb	hERG pIC_{50}	PSA[b]	cLogD[c]
37	phenyl (rac)	7.9	6.7	6.8	5.8	60	1.0
38	4-*t*-Bu (rac)	9.1	7.1	< 5.6	6.2	60	3.0
39	4-*t*-Bu (se)	8.5	< 6.0	6.6	6.4	60	3.0
40	4-*t*-Bu (se)	9.5	7.1	6.3	6.0	60	3.0
41	4-Br (rac)	8.7	6.9	7.9	6.4	60	2.2
42	4-Br (se)	9.4	6.9	8.1	6.3	60	2.2
43	4-Br (se)	6.4	< 5.9	6.0	6.1	60	2.2
44	4-OMe (rac)	8.3	6.9	< 5.5	5.9	69	1.1
45	4-OMe (se)	8.7	6.6	6.0	5.7	69	1.1
46	4-OMe (se)	7.0	< 5.8	6.0	5.6	69	1.1
47	3-OMe (rac)	8.1	6.3	6.3	5.8	69	1.0
48	3-OMe (se)	9.0	7.0	6.6	5.4	69	1.0
49	3-OMe (se)	6.6	< 6.4	< 5.5	5.2	69	1.0
50	4-Cl (rac)	8.9	6.5	6.4	6.1	60	1.9
51	4-Cl (se)	9.4	6.8	7.2	6.4	60	1.9
52	4-Cl (se)	6.3	< 6.2	8.0	6.1	60	1.9
53	3-Cl (rac)	8.3	7.0	6.9	5.8	60	1.9
54	3-Cl (se)	9.1	7.3	7.2	6.5	60	1.9
55	3-Cl (se)	7.9	6.3	6.5	5.9	60	1.9
56	4-F (rac)	8.2	6.3	7.8	5.7	60	1.3
57	4-F (se)	8.1	6.4	6.6	6.5	60	1.3
58	4-F (se)	6.3	6.5	7.7	5.7	60	1.3
59	3-F (rac)	8.3	6.7	7.4	5.7	60	1.0
60	3-F (se)	8.3	6.8	6.7	6.0	60	1.0
61	3-F (se)	6.4	< 6.2	6.1	6.0	60	1.0
62	3-CF_3 (rac)	9.3	7.5	5.6	5.5	60	1.8
63	3-CF_3 (se)	9.3	7.5	6.2	5.1	60	1.8
64	3-CF_3 (se)	7.8	< 6.4	7.1	5.6	60	1.8
65	2-CF_3 (rac)	7.5	< 6.1	6.1	5.2	60	2.4
66	4-OCF_3 (rac)	8.7	< 6.4	7.4	6.7	69	2.4
67	4-OCF_3 (se)	9.0	6.8	6.1	6.6	69	2.4
68	4-OCF_3 (se)	7.3	6.0	6.5	6.5	69	2.4
69	3,4-diCl (rac)	8.5	7.9	7.1	6.0	60	2.8
70	3,4-diCl (se)	9.0	7.5	6.3	6.3	60	2.8
71	3,4-diCl (se)	7.6	5.8	7.9	6.0	60	2.8
72	2-F, 4-CF_3 (rac)	8.8	6.6	< 5.5	6.0	60	2.9
73	2-F, 4-CF_3 (se)	6.9	< 6.2	6.3	6.3	60	2.9
74	2-F, 4-CF_3 (se)	8.9	6.2	5.7	6.1	60	2.9
75	2-Me, 4-CF_3 (rac)	7.0	< 6.0	6.0	6.4	60	2.6
76	3-CF_3, 4-F (rac)	8.9	7.0	6.3	5.7	60	2.5
77	3-CF_3, 4-F (se)	9.6	7.5	6.4	5.6	60	2.5
78	3-CF_3, 4-F (se)	7.1	6.0	6.6	6.3	60	2.5
79	2-F, 5-CF_3 (rac)	8.8	6.1	7.3	5.9	60	2.4
80	2-F, 5-CF_3 (se)	6.9	< 6.1	< 5.7	5.4	60	2.4
81	2-F, 5-CF_3 (se)	8.4	6.8	< 5.5	5.0	60	2.4
82	2-F, 3-CF_3 (rac)	9.1	6.9	6.5	6.0	60	2.8
83	2-F, 3-CF_3 (se)	7.2	6.6	6.5	5.5	60	2.8
84	2-F, 3-CF_3 (se)	8.9	7.2	6.2	5.4	60	2.8
85	3-F, 4-CF_3 (rac)	9.2	6.2	5.8	6.4	60	2.3
86	3-F, 4-CF_3 (se)	9.3	7.1	6.7	6.2	60	2.3
87	3-F, 4-CF_3 (se)	6.7	< 6.2	7.3	6.2	60	2.3
88	3-F, 5-CF_3 (rac)	9.2	7.5	7.2	6.0	60	1.8
89	3-F, 5-CF_3 (se)	9.1	7.9	NT	5.7	60	1.8
90	3-F, 5-CF_3 (se)	7.6	< 6.4	7.1	5.7	60	1.8
91	2-F, 4-Me (rac)	7.1	< 6.2	6.1	5.2	60	2.0
92	2-F, 4-Me (se)	< 6.2	< 6.1	5.6	6.0	60	2.0
93	2-F, 4-Me (se)	8.0	6.2	6.5	4.4	60	2.0
94	2-F, 4-Cl (rac)	8.2	< 6.2	7.3	6.3	60	2.7
95	2-F, 4-Cl (se)	6.5	< 6.1	5.5	6.0	60	2.7
96	2-F, 4-Cl (se)	8.6	6.5	7.2	6.4	60	2.7
97	3-CF_3, 4-OMe (rac)	8.9	6.8	7.0	5.9	69	1.9

Table 3. Continued

entry	R	hD_3-GTPγS fpK_i	hD_2-GTPγS fpK_i	hH_1-FLIPR pKb	hERG pIC_{50}	PSA[b]	cLogD[c]
98	3-CF_3, 4-OMe (se)	6.7	< 6.3	< 5.6	5.9	69	1.9
99	3-CF_3, 4-OMe (se)	8.9	6.6	7.4	5.9	69	1.9
100	3-Cl, 4-OMe (rac)	8.3	6.3	6.9	5.4	69	1.9
101	3-Cl, 4-OMe (se)	8.5	6.4	6.8	5.7	69	1.9
102	3-Cl, 4-OMe (se)	6.7	< 6.1	5.9	6.1	69	1.9
103	3-OCF_3 (rac)	8.8	6.8	6.6	6.2	69	2.3
104	3-OCF_3 (se)	7.3	< 6.1	< 5.5	6.0	69	2.3
105	3-OCF_3 (se)	9.0	7.7	6.5	6.0	69	2.3

[a] fpK_i = functional pK_i obtained from the GTPγS functional assay. FLIPR = fluorescent imaging plate reader. SEM for D_3 GTPγS, H1 FLIPR, and HERG data sets is ±0.1 and for the D_2 GTPγS data is ±0.2. [b] Å^2. [c] ACD logD 7.4. version 11.

less bulky than the hydrogen one), which is instead well tolerated. These results were confirmed by the general trend of the DA D_3 activity vs Daylight's ClogD, which is reported in Figure 3B. Among the few outliers which can be observed in this plot, derivatives **65** and **75** are endowed with RG-R2s carrying a bulky substituent in ortho (their Hansch's MR values are respectively 5.02 and 5.65), while all the other compounds have either a hydrogen or a fluorine in the ortho positions (with their Hansch MR values equal to 1.03 and 0.92, respectively). Derivative **17** contains a *p*-cyano-phenyl in RG-R2. Although the global polarity of the compound, as expressed by tPSA, is not much higher than that for the other molecules in the data set, this substituent is by far the most polar RG-R2. Potentially, very polar substituents might not be tolerated in this precise position in this specific series, although this hypothesis must be further explored. Finally, for derivative **9**, the theory previously discussed about a potential steric clash might be invoked; nonetheless, at the current status of the exploration, it is not possible to exclude any a priori hypothesis, including a potentially slightly different binding mode to the receptor within the subseries. As far as derivative **7** is concerned, the lack of substituents on the aryl ring, also in this case, might lead to a slightly different behavior.

When the analysis was repeated with respect to the hERG activity, it was evident that substituents on the right-hand side which were very efficient in boosting the DA D_3 activity (e.g., the furan and the 2-methyl-5-quinoline) were unfortunately also good at increasing hERG. However, the RG-R2 plot suggests that there was slight room for a divergent SAR for the two targets as reported in Figure 3C. The selection of the few compounds along the screening cascade and the use of receptor modeling techniques confirmed this possibility.

Further Characterization of Derivatives 27, 28, 32, 35, 51, and 74. In agreement with the screening cascade, these selected compounds underwent a further in vitro characterization enlarging the selectivity panel using both in-house testing and a selectivity screen available at Cerep as previously described.[7] Because the compounds showed at least 100-fold selectivity over a wide range of receptors and enzymes, they were submitted to a patch clamp hERG electrophysiology assay[7,16] to assess their overall activity for this K^+ channel. The results of the experiments are reported in Table 4.

On the basis of these new generated data, which considered the affinity at the DA D_3 receptor, the overall in vitro and in vivo PK properties of these derivatives and the in vivo efficacy of DA D_3 receptor antagonists in animal models of addiction[6] combined with our previous experience,[7] it was decided to temporarily remove derivatives **35** and **51** from further progression and to assess the efficacy of the remaining compounds in the expression of either nicotine or cocaine-induced conditioned place preference[7] (CPP).

Prior to these in vivo experiments, and for a better final interpretation of the results, it was also decided to generate affinity data in rat native tissues using [^{125}I]-7-OH-PIPAT in competition binding assays on brain homogenates from rat nucleus accumbens and olfactory tubercles; results from these experiments are reported in Table 5.

In the CPP paradigm, animals are given an injection of a drug or vehicle and confined or "paired" to a specific environment with distinct cues. This pairing of the animal with specific cues after being given vehicle or drug is repeated. Subsequently, on the test day, animals are not given any treatment (drug-free state) and are allowed to freely explore the CPP apparatus to determine if they prefer an environment in which they previously received drug compared to an environment in which they previously received vehicle. If the animals approach and spend a significantly greater amount of time in the drug-paired environment, one can reasonably infer that the drug was rewarding. Further details on this paradigm can be found in the experimental part.

Separate studies were performed to investigate the effects of the acute administration of derivatives **27**, **28**, **32**, and **74** compared to vehicle on the expression of nicotine CPP in male Sprague−Dawley rats. All the compounds were administered ip (0.05, 0.1, 0.3, 1.0, 3.0 mg/kg) and the amount of time spent in each chamber was determined using an automated timing system. The results are reported in Tables 6−9.

In addition, to further strengthen the available results[6] indicating that antagonism at the DA D_3 receptor is efficacious in attenuating the rewarding/reinforcing properties of different drugs of abuse, two of these four derivatives (namely **28** and **74**), were also tested to investigate their acute effects on the expression of cocaine CPP in male Sprague−Dawley rats. Both compounds were given ip (0.05, 0.1, 0.3, 1.0, 3.0 mg/kg). The results of these experiments are reported in Tables 10 and 11.

A one-way ANOVA revealed a significant main effect of dose on the time spent in the nicotine or cocaine-paired compartments, and the results clearly show that all the compounds tested significantly reduced both nicotine- (Table 6−9) and cocaine-induced CPP (Table 10−11) in a dose-dependent manner.

Additional experiments were performed to assess whether or not these derivatives produced nonspecific behavioral effects. Subsequently, the acute effects of these compounds up to high exposure (i.e., 10 mg/kg ip) were determined using spontaneous locomotor activity and motor coordination using the accelerating rotarod. For locomotor activity assessment, rats were treated with either saline or the test

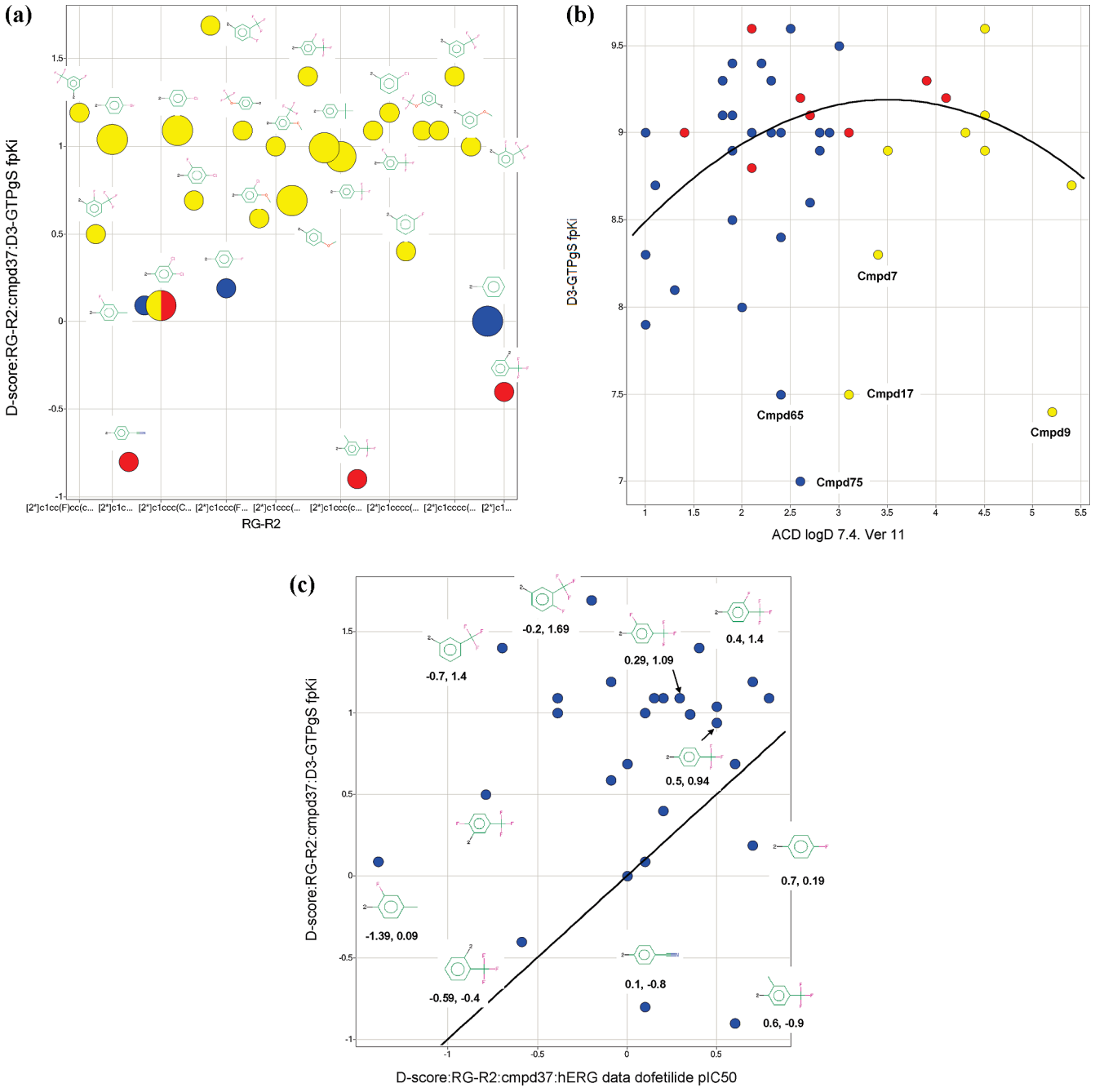

Figure 3. (A) Pie chart for RG-R2 fragmentation. See text for a comprehensive explanation of the technique. (B) General trend of DA D3 fpK_i vs whole molecule lipophilicity expressed as ACD logD 7.4. Ver 11. Dots are color coded according to RG-R1: yellow, quinoline series (Table 1); blue, oxazolo series (Table 3); red, other substituents (Table 2). (C) RG-R2 D-scores for hERG vs RG-R2 D-scores for D_3. Labels beneath the substituents are respectively D-score hERG, D-score D_3. RG-R2 groups positioned above the unity line have on average a greater effect on D_3 than on hERG.

Table 4. Results from Patch Clamp hERG Electrophysiology Assay for the Selected Derivatives[a]

compd	27	28	32	35	51	74
affinity at the hERG channel (μM)	0.39	0.47	0.35	0.20	0.11	0.46

[a] Results are expressed in μM values.

Table 5. Profile of the Selected Derivatives in [^{125}I]-7-OH-PIPAT Competition Binding Assay on Brain Homogenates from Rat Brain

compd	27	28	32	35	51	74
r DA D_3 rat native tissue pK_i	9.01	8.70	9.19	9.05	NT	8.38

compounds (1, 3, 10 mg/kg ip). All rats were subsequently placed in an AccuScan locomotor apparatus. Their locomotor activity was measured for a 30 min period. An overall ANOVA revealed that there was no significant effect of treatment and no significant treatment × time interval interaction (data not shown).

For motor coordination assessment, rats were trained on the accelerating rotarod (4−40 rpm over 270s; 7750, Ugo Basile, Italy) twice daily for 3 consecutive days. On the test day (day 4), rats were treated with vehicle, the four selected compounds (1, 3, 10 mg/kg ip), or haloperidol (1 mg/kg ip) as a positive control (n = 8 rats/group). Rats were then repeatedly tested for their endurance performance on the

Table 6. Effect of a Single ip Administration of Vehicle and **27** (0.05, 0.1, 0.3, 1, 3 mg/kg) on the Expression of the Conditioned Place Preference Response to 0.6 mg/kg sc of (−)-Nicotine or Vehicle (1 mL/kg sc) in Adult Male Sprague−Dawley Rats

		time spent in compartments (min) ± SEM	
treatment pairings	drug given on test day	paired	unpaired
vehicle/vehicle	vehicle	7.51 ± 0.3	7.49 ± 0.3
vehicle/nicotine	vehicle	9.81 ± 0.3[a]	5.19 ± 0.3
vehicle/nicotine	**27** (0.05 mg/kg)	9.73 ± 0.4	5.27 ± 0.4
vehicle/nicotine	**27** (0.1 mg/kg)	9.87 ± 0.4	5.13 ± 0.3
vehicle/nicotine	**27** (0.3 mg/kg)	9.55 ± 0.4	5.45 ± 0.4
vehicle/nicotine	**27** (1.0 mg/kg)	7.91 ± 0.3[b]	7.09 ± 0.3
vehicle/nicotine	**27** (3.0 mg/kg)	7.77 ± 0.4[b]	7.23 ± 0.4

[a] $P < 0.0001$ vs vehicle/vehicle/vehicle. [b] $P < 0.0001$ vs vehicle/nicotine/vehicle.

Table 7. Effect of a Single ip Administration of Vehicle and **28** (0.05, 0.1, 0.3, 1, 3 mg/kg) on the Expression of the Conditioned Place Preference Response to 0.6 mg/kg sc of (−)-Nicotine or Vehicle (1 mL/kg sc) in Adult Male Sprague−Dawley Rats

		time spent in compartments (min) ± SEM	
treatment pairings	drug given on test day	paired	unpaired
vehicle/vehicle	vehicle	7.51 ± 0.4	7.49 ± 0.4
vehicle/nicotine	vehicle	9.87 ± 0.4[a]	5.13 ± 0.4
vehicle/nicotine	**28** (0.05 mg/kg)	9.59 ± 0.4	5.41 ± 0.4
vehicle/nicotine	**28** (0.1 mg/kg)	9.14 ± 0.4	5.86 ± 0.4
vehicle/nicotine	**28** (0.3 mg/kg)	8.49 ± 0.4[b]	6.51 ± 0.4
vehicle/nicotine	**28** (1.0 mg/kg)	7.65 ± 0.4[c]	7.35 ± 0.4
vehicle/nicotine	**28** (3.0 mg/kg)	7.10 ± 0.3[c]	7.90 ± 0.3

[a] $P < 0.0001$ vs vehicle/vehicle/vehicle. [b] $P < 0.001$ vs vehicle/nicotine/vehicle. [c] $P < 0.0001$ vs vehicle/nicotine/vehicle.

Table 8. Effect of a Single ip Administration of Vehicle and **32** (0.05, 0.1, 0.3, 1, 3 mg/kg) on the Expression of the Conditioned Place Preference Response to 0.6 mg/kg sc of (−)-Nicotine or Vehicle (1 mL/kg sc) in Adult Male Sprague−Dawley Rats

		time spent in compartments (min) ± SEM	
treatment pairings	drug given on test day	paired	unpaired
vehicle/vehicle	vehicle	7.41 ± 0.4	7.49 ± 0.4
vehicle/nicotine	vehicle	9.82 ± 0.3[a]	5.18 ± 0.3
vehicle/nicotine	**32** (0.05 mg/kg)	9.58 ± 0.3	5.42 ± 0.4
vehicle/nicotine	**32** (0.1 mg/kg)	9.16 ± 0.2	5.84 ± 0.4
vehicle/nicotine	**32** (0.3 mg/kg)	8.23 ± 0.2[b]	6.77 ± 0.3
vehicle/nicotine	**32** (1.0 mg/kg)	7.54 ± 0.3[c]	7.46 ± 0.4
vehicle/nicotine	**32** (3.0 mg/kg)	7.16 ± 0.3[c]	7.84 ± 0.3

[a] $P < 0001$ vs vehicle/vehicle/vehicle. [b] $P < 001$ vs vehicle/nicotine/vehicle. [c] $P < 0001$ vs. vehicle/nicotine/vehicle.

rotarod 30, 60, and 120 min after these treatments. Rotarod latencies were measured with a 270 s cutoff time. Pretreatment with haloperidol significantly decreased the time that rats spent on the rotarod. In contrast, the selected derivatives (**27**, **28**, **32**, **74**) did not affect endurance performance at any of the posttreatment times tested (data not shown).

A final important point to be assessed in this quest for new and developable selective DA D_3 receptor antagonist, as it was done for the previously reported BAZ system,[7] was related to the demonstration of the lack of QTc prolongation in vivo. It is well-known that an undesirable feature of some drugs is their ability to delay cardiac repolarization, an effect

Table 9. Effect of a Single ip Administration of Vehicle and **74** (0.05, 0.1, 0.3, 1, 3 mg/kg) on the Expression of the Conditioned Place Preference Response to 0.6 mg/kg sc of (−)-Nicotine or Vehicle (1 mL/kg sc) in Adult Male Sprague−Dawley Rats

		time spent in compartments (min) ± SEM	
treatment pairings	drug given on test day	paired	unpaired
vehicle/vehicle	vehicle	7.51 ± 0.3	7.49 ± 0.3
vehicle/nicotine	vehicle	9.39 ± 0.4[a]	5.61 ± 0.4
vehicle/nicotine	**74** (0.05 mg/kg)	8.68 ± 0.3	6.32 ± 0.3
vehicle/nicotine	**74** (0.1 mg/kg)	8.07 ± 0.3[b]	6.93 ± 0.3
vehicle/nicotine	**74** (0.3 mg/kg)	7.42 ± 0.3[c]	7.58 ± 0.3
vehicle/nicotine	**74** (1.0 mg/kg)	7.26 ± 0.2[c]	7.84 ± 0.2
vehicle/nicotine	**74** (3.0 mg/kg)	7.05 ± 0.2[c]	7.95 ± 0.2

[a] $P < 0001$ vs vehicle/vehicle/vehicle. [b] $P < 001$ vs vehicle/nicotine/vehicle. [c] $P < 0001$ vs vehicle/nicotine/vehicle.

Table 10. Effect of a Single ip Administration of Vehicle and **28** (0.05, 0.1, 0.3, 1, 3 mg/kg) on the Expression of the Conditioned Place Preference Response to 15 mg/kg ip of (−)-Cocaine or Vehicle (1 mL/kg sc) in Adult Male Sprague−Dawley Rats

		time spent in compartments (min) ± SEM	
treatment pairings	drug given on test day	paired	unpaired
vehicle/vehicle	vehicle	7.11 ± 0.4	7.90 ± 0.4
vehicle/cocaine	vehicle	10.83 ± 0.5[a]	4.17 ± 0.5
vehicle/cocaine	**28** (0.05 mg/kg)	9.79 ± 0.3[b]	5.21 ± 0.3
vehicle/cocaine	**28** (0.1 mg/kg)	9.36 ± 0.4[c]	5.64 ± 0.4
vehicle/cocaine	**28** (0.3 mg/kg)	8.70 ± 0.5[d]	6.30 ± 0.5
vehicle/cocaine	**28** (1.0 mg/kg)	7.89 ± 0.3[d]	7.11 ± 0.3
vehicle/cocaine	**28** (3.0 mg/kg)	7.36 ± 0.3[d]	7.64 ± 0.3

[a] $P < 0001$ vs vehicle/vehicle/vehicle. [b] $P < 05$ vs vehicle/cocaine/vehicle. [c] $P < 01$ vs vehicle/nicotine/vehicle. [d] $P < 0001$ vs vehicle/nicotine/vehicle.

Table 11. Effect of a Single ip Administration of Vehicle and **74** (0.05, 0.1, 0.3, 1, 3 mg/kg) on the Expression of the Conditioned Place Preference Response to 15 mg/kg ip of (−)-Cocaine or Vehicle (1 mL/kg sc) in Adult Male Sprague−Dawley Rats

		time spent in compartments (min) ± SEM	
treatment pairings	drug given on test day	paired	unpaired
vehicle/vehicle	vehicle	7.06 ± 0.4	7.94 ± 0.4
vehicle/cocaine	vehicle	10.81 ± 0.5[a]	4.19 ± 0.5
vehicle/cocaine	**74** (0.05 mg/kg)	10.44 ± 0.4	4.56 ± 0.4
vehicle/cocaine	**74** (0.1 mg/kg)	9.01 ± 0.4[b]	5.89 ± 0.4
vehicle/cocaine	**74** (0.3 mg/kg)	8.23 ± 0.3[c]	6.87 ± 0.3
vehicle/cocaine	**74** (1.0 mg/kg)	7.56 ± 0.3[c]	7.34 ± 0.3
vehicle/cocaine	**74** (3.0 mg/kg)	7.10 ± 0.3[c]	7.90 ± 0.3

[a] $P < 0001$ vs vehicle/vehicle/vehicle. [b] $P < 001$ vs vehicle/nicotine/vehicle. [c] $P < 0001$ vs vehicle/nicotine/vehicle.

that can be measured as prolongation of the QT interval on the surface electrocardiogram (ECG).[17,18] Because of its inverse relationship to heart rate, the QT interval is routinely transformed (normalized) by means of various formulas into a heart rate independent "corrected" value known as the QTc interval. The QTc interval is intended to represent the QT interval at a standardized heart rate of 60 bpm.

In agreement with our screening cascade, derivatives **27**, **28**, **32**, and **74** were all evaluated for their ability to determine QTc prolongation in vivo when assessed in the anesthetized guinea pig model.[19] All of the compounds were administered

intravenously in escalating doses from 0.5 to 15 mg/kg. Despite the very high exposure reached at the top dose of 15 mg/kg (C_{max} = 6237, 9577, 8322, and 8635 ng/mL for **27**, **28**, **32**, and **74**, respectively), the QTc interval was not significantly increased in the guinea pig model by any of the derivatives. Thus, there is a large window between the efficacy and the potential side effects that was obtained in preclinical species for these derivatives.

Conclusions

Starting from the potent and selective DA D_3 receptor antagonists previously reported (**1**−**4**), a new series of 1,2,4-triazol-yl azabicyclo[3.1.0]hexanes was identified. Rational design and computational tools helped to design a number of products endowed with high affinity and selectivity for the DA D_3 receptor. In addition, selected compounds of this family series proved to have appropriate developability characteristics (P450, Cl_i, F%) and good CNS penetration. As described, a number of these compounds were also active in the CPP model and were endowed with a large selectivity window with respect to their affinity at the hERG channel, leading to a total lack of QTc when assessed in vivo in the anesthetized guinea pig model.

Provided that in vivo preclinical evidence can be extrapolated to human, selective DA D_3 receptor antagonists belonging to this new chemical series show high promise for the treatment of drug addiction.

Experimental Section

Biological Test Methods. In Vitro Studies. [^{35}S] GTPγS Functional Binding Assay in Cell Membranes Expressing hD_3 Receptors. In vitro functional studies were performed according to the following [^{35}S]-GTPγS protocol. Cells used in the study are Chinese hamster ovary (CHO) cells.

Cell membranes were prepared as follows. Cell pellets were resuspended in 10 volumes of 50 mM HEPES, 1 mM EDTA pH 7.4, using KOH. On the day, the following proteases were added to the buffer just prior to giving the homogenization buffer.

10−6 M leupeptin (Sigma L2884) − 5000 × stock = 5 mg/mL in buffer.

25μg/mL bacitracin (Sigma B0125) − 1000 × stock = 25 mg/mL in buffer.

1 mM PMSF − 1000 × stock = 17 mg/mL in 100% ethanol.

2×10^{-6} M pepstain A − 1000 × stock = 2 mM in 100% DMSO.

The cells were homogenized by 2 × 15 s bursts in a 1 L glass Waring blender in a class two biohazard cabinet. The resulting suspension was spun at 500g for 20 min (Beckman T21 centrifuge: 1550 rpm). The supernatant was withdrawn with a 25 mL pipet, aliquotted into prechilled centrifuge tubes, and spun at 48000g to pellet membrane fragments (Beckman T1270: 23000 rpm for 30 min). The final 48000g pellet was resuspended in homogenization buffer (4× the volume of the original cell pellet). The 48000g pellet was resuspended by vortexing for 5 s and homogenized in a dounce homogenizer 10−15 stokes. The prep was distributed into appropriate sized aliquots (200−1000 μL) in polypropylene tubes and store at −800 °C. Protein content in the membrane preparations was evaluated with the Bradford protein assay.

The final top concentration of test drug was 3 μM in the assay, and 11 points serial dilution curves 1:4 in 100% DMSO were carried out using a Biomek FX. The test drug at 1% total assay volume (TAV) was added to a solid, white, 384-well assay plate. 50%TAV of precoupled (for 90 min at 4 °C) membranes, 5 μg/well, and wheatgerm agglutinin polystyrene scintillation proximity assay beads (RPNQ0260, Amersham), 0.25 mg/well, in 20 mM HEPES pH 7.4, 100 mM NaCl, 10 mM $MgCl_2$, 60 μg/mL saponin, and 30 μM GDP is added. The third addition was a 20% TAV addition of either buffer (agonist format) or EC_{80} final assay concentration of agonist, Quinelorane, prepared in assay buffer (antagonist format). The assay was started by the addition of 29%TAV of GTPγ[35S] 0.38 nM final (37 MBq/mL, 1160 Ci/mmol, Amersham). After all additions assay plates were spun down for 1 min at 1000 rpm, assay plates were counted on a Viewlux, 613/55 filter, for 5 min, between 2 and 6 h after the final addition.

The effect of the test drug over the basal generates EC_{50} value by an iterative least-squares curve fitting program, expressed in the table as pEC_{50} (i.e., $-\log EC_{50}$). The ratio between the maximal effect of the test drug and the maximal effect of full agonist, Quinelorane, generated the intrinsic activity (IA) value (i.e., IA = 1 full agonist, IA < 1 partial agonist). fpK_i values of test drug were calculated from the IC_{50} generated by "antagonist format" experiment using Cheng and Prusoff equation: $fK_i = IC_{50}/1 + ([A]/EC_{50})$, where [A] is the concentration of the agonist in the assay and EC_{50} is the agonist EC_{50} value obtained in the same experiment. fpK_i is defined as $-\log fK_i$.

[^{125}I]-7-OH-PIPAT Competition Bbinding Assay on Brain Homogenates from Rat Brain. Homogenates from frozen nucleus accumbens and olfactory tubercles were prepared as described by Burris et al. (1994).[20] In saturation experiments, increasing concentrations of [^{125}I]-7-OH-PIPAT (15 pM−2 nM) were incubated with 12 μg/well of homogenates for 45 min at 37 °C in a final volume of 200 μL of 50 mM Tris-HCl (pH7.0), 50 mM NaCl, 100 μM Gpp(NH)p, and 0.02%BSA, i.e., conditions which inhibit [^{125}I]-7-OH-PIPAT binding to D_2 and $5HT_{1A}$ receptors.[20] Nonspecific binding was determined by the presence of 1 μM **1**. In competition binding experiments, increasing concentrations of **35** (17 pM−1 μM) were incubated as above in the presence of 0.1 nM [^{125}I]-7-OH-PIPAT.

Reactions were stopped by filtration through GF/C 96-well filter plates presoaked in 0.3% polyethylenimine using a cell harvester. Filters were washed 3 times with 1 mL of ice-cold 50 mM Tris-HCl (pH7.7), and radioactivity was counted in a microplate scintillation counter (Top Count, Perkin-Elmer).

Radioligand binding data were analyzed by nonlinear regression analysis using GraphPad Prism 4.0 (GraphPad Software, CA). Determination of K_D and B_{max} of [^{125}I]-7-OH-PIPAT from saturation experiments was assessed by using one-site binding (hyperbola) equation. Curve fitting from competition-binding experiments was determined by using one site competition equation after checking with F test ($P < 0.05$) that Hill slope in the four parameter logistic equation was not statistically different from 1.0. In this condition, IC_{50} values were converted to K_i using the Cheng−Prusoff equation.[33] Results are expressed as mean $pK_i \pm$ SEM.

[^{125}I]-7-OH-PIPAT ([^{125}I](*R*)-*trans*-7-hydroxy-2-[*N*-propyl-*N*-(3′-iodo-2′-propenyl)amino] tetralin, 81.4 TBq/mmol) was purchased from PerkinElmer Life and Analytical Sciences. Haloperidol and Gpp(NH)p (guanylyl-5′-imidodiphosphate) were obtained from Sigma Chemicals.

hERG-^{3}H Dofetilide Binding Assay. hERG activity was measured using ^{3}H dofetilide binding in a scintillation proximity assay (SPA) format. The activity was measured with a Perkin-Elmer Viewlux imager.

H1-FLIPR Assay. A functional response in CHO-hH1 cells was measured using cytoplasmic calcium indicator, Fluo-4. The change in cell fluorescence was measured in a FLIPR (λ_{ex} = 488 nm, λ_{EM} = 540 nm, Molecular Devices, UK).

P450 CYPEX Assay. Inhibition (IC_{50}) of human CYP1A2, 2C9, 2C19, 2D6, and 3A4 was determined using Cypex Bactosomes expressing the major human P450s. A range of concentrations (0.1, 0.2, 0.4, 1, 2, 4, and 10 μM) of test compound were prepared in methanol and preincubated at 37 °C for 10 min in 50 mM potassium phosphate buffer (pH 7.4) containing recombinant human CYP450 microsomal protein (0.1 mg/mL; Cypex

Limited, Dundee, UK) and probe-fluorescent substrate. The final concentration of solvent was between 3 and 4.5% of the final volume. Following preincubation, NADPH regenerating system (7.8 mg glucose 6-phosphate, 1.7 mg NADP, and 6 units glucose-6-phosphate dehydrogenase/mL of 2% (w/v) NaHCO3; 25 μL) was added to each well to start the reaction. Production of fluorescent metabolite was then measured over a 10 min time-course using a Spectrafluor plus plate reader. The rate of metabolite production (AFU/min) was determined at each concentration of compound and converted to a percentage of the mean control rate using Magellan (Tecan software). The inhibition (IC_{50}) of each compound was determined from the slope of the plot using Grafit v5 (Erithacus software, UK). Miconazole was added as a positive control to each plate. CYP450 isoform substrates used were ethoxyresorufin (ER; 1A2; 0.5 μM), 7-methoxy-4-triflouromethylcoumarin-3-acetic acid (FCA; 2C9; 50 μM), 3-butyryl-7-methoxycoumarin (BMC; 2C19; 10 μM), 4-methylaminomethyl-7-methoxycoumarin (MMC; 2D6; 10 μM), diethoxyflourescein (DEF; 3A4; 1 μM), and 7-benzyloxyquinoline (7-BQ; 3A4; 25 μM). The test was performed in three replicates.

Intrinsic Clearance (Cl_i) Assay. Intrinsic clearance (CL_i) values were determined in rat and human liver microsomes. Test compounds (0.5 μM) were incubated at 37 °C for 30 min in 50 mM potassium phosphate buffer (pH 7.4) containing 0.5 mg microsomal protein/mL. The reaction was started by addition of cofactor (NADPH; 8 mg/mL). The final concentration of solvent was 1% of the final volume. At 0, 3, 6, 9, 15, and 30 min, an aliquot (50 μL) was taken, quenched with acetonitrile containing an appropriate internal standard, and analyzed by HPLC-MS/MS. The intrinsic clearance (CL_i) was determined from the first-order elimination constant by nonlinear regression using Grafit v5 (Erithacus software, UK), corrected for the volume of the incubation and assuming 52.5 mg microsomal protein/g liver for all species. Values for CL_i were expressed as mL/min/g liver. The lower limit of quantification of clearance was determined to be when $< 15\%$ of the compound had been metabolized by 30 min and this corresponded to a CL_i value of 0.5 mL/min/g liver. The upper limit was 50 mL/min/g liver.

Patch Clamp hERG Electrophysiology Assay. On the days of experimentation, a weighed amount of the test substance was formulated in dimethyl sulfoxide (DMSO, lot no. U10781; Sigma-Aldrich, UK) by shaking to give a stock concentration of 10 mM of the test compound. The 10 mM stock solution was serially diluted in DMSO to give further stock solutions of 1 and 0.1 mM. Aliquots of these stock solutions were added to bath solution to achieve final perfusion concentrations of 0.1, 1, and 10 μM test compound. The corresponding vehicle concentration in all test substance perfusion solutions was 0.1% DMSO. Test substance stock formulations were freshly prepared on each day of experimentation, stored at room temperature, and protected from light.

Reference Substance. E-4031 (batch no. MLE9446; Wako Pure Chemical Industries Ltd.). Stock solutions of E-4031 (100 μM) were prepared in reverse osmosis water, aliquoted, and stored at approximately −20 °C until use. On the day of use, the 100 μM stock solution was added to bath solution to give a final perfusion concentration of 100 nM.

Bath and Pipette Solutions. The composition of bath solution was (mM): NaCl 137, KCl 4, $CaCl_2$ 1.8, $MgCl_2$ 1.0, D-glucose 10, *N*-2-hydroxyethylpiperazine-*N*′-2-ethanesulfonic acid (HEPES) 10, pH 7.4 with 1 M NaOH. Pipette solution was prepared in batches, aliquoted, and stored frozen until the day of use. The composition of pipet solution was (mM): KCl 130, $MgCl_2$ 1.0, ethylene glycol-bis(ss-aminoethyl ether)-*N*,*N*,*N*′,*N*′-tetraacetic acid (EGTA) 5, MgATP 5, HEPES 10, pH 7.2, with 1 M KOH.

Study Design. Cells (passage number: 48) were transferred to the recording chamber and continuously perfused (at approximately 1−2 mL/min) with bath solution at room temperature. High resistance seals (seal resistances > 1.5 GΩ) were formed between the patch electrodes (resistance range: 1.4−5.5 MΩ) and individual cells. The membrane across the electrode tip was then ruptured and the whole-cell patch-clamp configuration was established. Once a stable patch had been achieved, recording commenced in voltage-clamp mode, with the cell initially clamped at −80 mV. Currents were evoked by stepping the membrane potential to +20 mV and then to −50 mV (tail current). Test compound at 10, 1, and 0.1 μM was used to produce (if any) inhibition of hERG tail current and therefore to investigate the concentration−response relationship (n = 3 cells/concentration). The effect of the vehicle (0.1% DMSO) was investigated in 3 cells. The effect of 100 nM E-4031 was investigated in 2 of the vehicle treated cells to confirm the sensitivity of the test system to an agent known to block hERG current. All perfusion solutions were applied for approximately 10 min.

Anesthetized Guinea Pig Model for the Assessment of QT Prolongation. Prior to the experiment, six male Hartley guinea pigs (Charles River, France) weighing between 564 and 605 g on the day of the test were anaesthetised with urethane (1−1.5 g/kg ip), tracheotomized, artificially ventilated with a tidal volume of approximately 1 mL/100 g at a rate of 54 cycles/min, and surgically prepared for the experiment (i.e., insertion of catheters in appropriate blood vessels, see below, and placement of surface electrodes for lead II electrocardiogram recording). The animal's temperature was kept constant between 36.8 and 38.0 °C. Once physiological parameters were stabilized (approximately 30 min following surgery), each animal was given either the vehicle (5% w/v dextrose in aqueous 0.9 w/v sodium chloride) or test compound by the intravenous route (via the jugular vein) over 15 min/treatment.

The following parameters were recorded: arterial pressure (via the carotid artery), heart rate, electrocardiography (i.e., RR, PQ, QRS, and QT interval duration; the QT interval was corrected for heart rate changes according to Fridericia, Bazett and Van de Water's formula). Parameters were recorded prior to dosing to establish baseline measurements and continuously during the infusion period but data were reported every 5 min during each infusion period. In addition, blood samples (0.3 mL) were collected via the femoral artery at the end of each infusion period for toxicokinetic evaluations.

In Vivo Studies. All experiments were prereviewed and approved by a local animal care committee in accordance with the guidelines of the "Principles of Laboratory Animal Care" (NIH publication no. 86-23, revised 1985) and with a project license that was obtained according to Italian law (Art. 7, Legislative Decree no. 116, 27 January 1992), which acknowledges European Directive 86/609/EEC on the care and welfare of laboratory animals.

Nicotine CPP. Male Sprague−Dawley rats (200 g at the start of the pairings, Taconic Farms, Germantown, NY) were used in all experiments. Animals were housed two per cage, and there was no more than a 5% difference in body weight between the cagemates. Animals were kept on a 12 h lights on/12 h lights off schedule (lights on at 09.00 h). Food and water were freely available. The conditioning and testing of all animals was carried out between 11.00−18.00 h. All rats were naive and used only once.

An automated, two-chambered, Plexiglas CPP apparatus was used as previously described,[21−23] with modifications. Briefly, the two pairing chambers of the apparatus were identical in dimensions (25 cm × 14 cm × 36 cm) and were separated by removable Plexiglas guillotine doors. The pairing chambers were composed of distinct visual and tactile cues. The walls of one of the pairing chambers were white, with cage bedding on the floor and the walls of the second chamber consisted of alternating white and black boxes (1.2 cm × 1.8 cm) in a chessboard pattern and a Plexiglas floor. The two pairing chambers were separated by a third, neutral connecting tunnel, with one-half of the wall white and the other half with black and white boxes.

Expression studies with the compounds reported in the tables or vehicle were divided into four phases: acclimation, handling, conditioning, and testing. The animals were not exposed to the chambers prior to the start of the pairings. During days 1−3, animals were acclimated to the animal facility. During handling (days 4−6), animals were transported to the laboratory and handled for 5 min each. During conditioning (days 7−14), animals were exposed to once-daily conditioning sessions. For each conditioning session, animals (10 rats per group) were injected with nicotine (0.6 mg/kg sc in a volume of 1 mL/kg) or vehicle (1 mL/kg sc) and then immediately confined for 30 min in an appropriate cue-specific chamber. During conditioning, nicotine was always paired with 1 cue-specific environment, and vehicle was paired with the other; nicotine or vehicle exposure (and appropriate environmental pairing) alternated from day to day. This was done over an 8-day period, i.e., animals were given four pairings with nicotine and there was a 24 h separation between exposure to vehicle and nicotine. The animals in each group were randomly assigned to a 2 × 2 factorial design, with one factor being the pairing chamber and the other factor being the order of conditioning. In the counterbalanced procedure, the animals were randomly assigned to one of the two pairing chambers so that half of the subjects received the drug in one compartment (white walls with bedding on the floor) and the other half in the other compartment (alternating black and white boxes with a smooth chamber floor). This procedure resulted in the animals receiving equal exposure to the two compartments and due to random assignment controlled for their side preference. Another group of 10 animals were paired with vehicle in both chambers of the apparatus. On the test day (day 15), animals were randomly divided into five groups of 10 and received the test compounds or vehicle (10% 2-hydroxypropyl-β-cyclodextrin) in the home cage 30 min before they were placed in the apparatus and allowed free access to both chambers for 15 min. The amount of time spent in each chamber was determined using an automated timing system.

(−)-Nicotine (+)-bitartrate salt was used in all experiments (Sigma-Aldrich Corporation, Saint Louis, MO) and was dissolved in sterile physiological saline and the pH adjusted to 7.4 with NaOH. The doses of nicotine were expressed as free base. 2-Hydroxypropyl-β-cyclodextrin was purchased from Tocris-Cookson Chemical (St. Louis, MO). Data were analyzed with a 1-way ANOVA with a main factor of dose. Statistical significance was set at a probability level of $P < 0.05$.

Cocaine CPP. The cocaine CPP procedure was identical to the one described for nicotine except that (1) only four pairings were used and (2) for each conditioning session, animals were injected with (−)-cocaine HCl (15 mg/kg ip in a volume of 1 mL/kg) or vehicle (1 mL/kg ip of deionized, distilled water). (−)-Cocaine HCl was purchased from Sigma Chemicals (St. Louis, MO).

Chemical Procedures. General. Experimental. NMR spectra were obtained on Varian INOVA spectrometers (300, 400, and 500 MHz). Chemical shifts are expressed in δ (ppm) units and peak multiplicity are expressed as follows: singlet (s), doublet (d), doublet of doublets (dd), triplet (t), multiplet (m), broad singlet (br s), broad multiplet (br m). All mass spectrometric measurements were performed using a Micromass Platform LCZ (Waters, Manchester, UK) mass spectrometer operated in positive electrospray ionization mode. When LC/MS detection was performed, analytical conditions were used as reported in Table 12.

General Synthetic Procedures. Appropriate 4-methyl-5-aryl-2,4-dihydro-3*H*-1,2,4-triazole-3-thiones, prepared by the aryl acid in agreement with literature procedures, were suspended in acetone and potassium carbonate and 1-bromo-3-chloropropane was added. The so obtained 3-[(3-chloropropyl)thio]-4-methyl-5-aryl-4*H*-1,2,4-triazoles were suspended/dissolved in dry acetonitrile or DMF and added (1*S*,5*R*/1*R*,5*S*) or (1*S*,5*R*) aryl azabicyclo[3.1.0]hexanes in presence of potassium carbonate according to Scheme 1.

Table 12

analytical column	Zorbax SB-C18, 4.6 mm × 50 mm (1.8 μ)
mobile phase	amm acet, 5 mM + 0.1% formic acid/acetonitrile + 0.1% formic acid
gradient	97/3 → 36/64 v/v in 3.5 min → 10/90 in 3.5 min
flow rate	2.0 mL/min
detection	DAD, 210−350 nm
MS	ES+

Crudes were evaporated and purified by column chromatography. The solids were taken up with dichloromethane and a 1.0 M HCl solution in diethylether was added; the solvent was removed under reduced pressure to give product compounds as hydrochloride salts.

Where no specific details are given, the retention times reported refer to the following general analytical chromatographic conditions of method A: column, X Terra MS C18 5 mm, 50 mm × 4.6 mm; mobile phase: A = NH_4HCO_3 soln 10n mM, pH 10; B = CH_3CN; gradient, 10% (B) for 1 min, from 10% (B) to 95% (B) in 12 min, 95% (B) for 3 min. Flow rate: 1 mL/min. UV wavelength range: 210−350 nm. Mass range: 100−900 amu. Ionization method: ES+

The enantiomeric purity of each single enantiomer obtained after preparative chromatography on chiral columns was always verified on analytical column. For example, enatiomeric excess has been measured on the separated enantiomers by means of SFC analytical techniques. Typical conditions were derived from Chiralpak AD-H column (25 cm × 0.46 cm) with ethanol (+0.1% isopropylamine) 15% as modifier, flow rate 2.5 mL/min, $P = 180$ bar at 35 °C with detection at 220 nm.

The purity of the compounds reported in the manuscript was established through HPLC methodology. All the compounds reported in the manuscript have a purity >95%.

2-Methyl-5-[4-methyl-5-({3-[(1*R*,5*S*/1*S*,5*R*)-1-phenyl-3-azabicyclo[3.1.0]hex-3-yl]propyl}thio)-4*H*-1,2,4-triazol-3-yl]quinoline Hydrochloride (5). The compound was obtained as a white, slightly hygroscopic, solid. ^{1}H NMR (1H, DMSO-d_6): δ: 10.4 (bs,1H), 8.3 (bs, 1H), 8.2 (d, 1H), 7.9 (t, 1H), 7.8 (d, 1H), 7.6 (bd, 1H), 7.4−7.3 (m, 5H), 4.0−3.5 (m/m, 2H), 3.7−3.45 (m/m, 2H), 3.5−3.3 (m, 7H), 2.73 (s, 3H), 2.3 (m, 3H), 1.60,1.1 (t,t 2H). MS: m/z 456 $[M + H]^+$.

Derivative **5** was separated to give the separated enantiomers by semipreparative HPLC. Retention times given were obtained using an analytical HPLC using a chiral column Chiralcel OD 5 μm, 250 mm × 4.6 mm; eluent A: *n*-hexane; B: 2-propanol, gradient isocratic 25% B, flow rate 1 mL/min, detection UV at 200−400 nm. Enantiomer **6** retention time = 39.2 min; enantiomer **7** retention time = 43.4 min.

5-[5-({3-[(1*R*,5*S*/1*S*,5*R*)-1-(3,4-Dichlorophenyl)-3-azabicyclo[3.1.0]hex-3-yl]propyl}thio)-4-methyl-4*H*-1,2,4-triazol-3-yl]-2-methylquinoline Hydrochloride (8). The compound was obtained as a white, slightly hygroscopic, solid (70% yield). ^{1}H NMR (1H, DMSO-d_6) δ: 10.46 (bs,1H), 8.58 (s, 1H), 7.4−7.2 (m, 5H), 4.04 (dd, 1H), 3.73 (m, 1H), 3.7 (s, 3H), 3.7−3.4 (m, 2H), 3.4−3.2 (m + t, 4H), 2.39 (s, 3H), 2.17 (m, 3H), 1.64,1.1 (2t, 2H). MS: m/z 562 $[M + H]^+$.

5-[5-({3-[(1*R*,5*S*/1*S*,5*R*)-1-(4-*tert*-Butylphenyl)-3-azabicyclo[3.1.0]hex-3-yl]propyl}thio)-4-methyl-4*H*-1,2,4-triazol-3-yl]-2-methylquinoline Hydrochloride (11). The compound was obtained as a white, slightly hygroscopic, solid. ^{1}H NMR (1H, DMSO-d_6): δ: 10.16 (bs,1H), 8.15 (dd, 2H), 7.89 (t, 1H), 7.76 (d, 1H), 7.49 (d, 1H), 7.36 (d, 2H), 7.23 (d, 2H), 4.05 (dd, 1H), 3.77 (dd, 1H), 3.58 (m, 2H), 3.44 (s, 3H), 2.7 (bm, 4H), 2.34 (s, 3H), 2.23 (t, 2H), 2.15 (t, 1H), 1.51 (t, 1H), 1.27 (s, 9H), 1.14 (m, 1H). MS: m/z 512 $[M + H]^+$.

Derivative **11** was separated to give the separated enantiomers by chiral chromatography. Retention times given were obtained using an analytical supercritical fluid chromatography (Gilson) using a chiral column Chiralpak AD-H, 25 cm × 0.46 cm, eluent CO_2 containing 20% (ethanol + 0.1% 2-propanol), flow rate 2.5 mL/min, P 194 bar, T 35 °C, detection UV at 220 nm. Enantiomer **12** retention time = 7.0 min; enantiomer **13** retention time = 7.8 min.

5-[5-({3-[(1*R*,5*S*/1*S*,5*R*)-1-(4-Bromophenyl)-3-azabicyclo[3.1.0]-hex-3-yl]propyl}thio)-4-methyl-4*H*-1,2,4-triazol-3-yl]-2-methylquinoline Hydrochloride (14). The compound was obtained as a white, slightly hygroscopic, solid. ^{1}H NMR (1H, DMSO-d_6) δ: 10.28 (bs,1H), 8.16 (dd, 2H), 7.89 (dd, 1H), 7.76 (d, 1H), 7.55 (d, 2H), 7.49 (d, 1H), 7.28 (d, 2H), 4.06 (bm, 1H), 3.77 (bm, 1H), 3.6 (bm, 2H), 3.44 (s, 3H), 3.5−3.2 (bm, 4H), 2.71 (s, 3H), 2.23 (m, 3H), 1.58/1.14 (t/m, 2H). MS: m/z 534 $[M + H]^+$.

Derivative **14** was separated to give the separated enantiomers. Retention times given were obtained using an analytical supercritical fluid chromatography (Gilson) using a chiral column Chiralcel OJ-H, 25 cm × 0.46 cm, eluent CO2 containing 10% (ethanol + 0.1% isopropylamine), flow rate 2.5 mL/min, *P* 196 bar, *T* 35 °C, detection UV at 220 nm. Enantiomer **15** retention time = 56.8 min; enantiomer **16**. Retention time = 62.5 min. The absolute configuration of enantiomer **15** was assigned using comparative VCD and comparative OR analyses of the corresponding free base to be 5-[5-({3-[(1*R*,5*S*)-1-(4-bromophenyl)-3-azabicyclo[3.1.0]hex-3-yl]propyl}thio)-4-methyl-4*H*-1,2,4-triazol-3-yl]-2-methylquinoline. The absolute configuration of enantiomer **16** was assigned as described above to be 5-[5-({3-[(1*S*,5*R*)-1-(4-bromophenyl)-3-azabicyclo[3.1.0]hex-3-yl]propyl}thio)-4-methyl-4*H*-1,2,4-triazol-3-yl]-2-methylquinoline.

Enantiomer **15**: specific optical rotation of the corresponding free base [α]D = +47° ($CHCl_3$, *T* = 20 °C, *c* = 0.066 g/mL).

Enantiomer **16**: specific optical rotation of the corresponding free base [α]D = −42° ($CHCl_3$, *T* = 20 °C, *c* = 0.065 g/mL).

4-[(1*R*,5*S*/1*S*,5*R*)-3-(3-{[4-Methyl-5-(2-methylquinolin-5-yl)-4*H*-1,2,4-triazol-3-yl]thio}propyl)-3-azabicyclo[3.1.0]hex-1-yl]-benzonitrile Hydrochloride (17). The compound was obtained as a white, slightly hygroscopic, solid. ^{1}H NMR (1H, DMSO-d_6) δ: 10.45 (bs,1H), 8.26 (bd, 1H), 8.17 (d, 1H), 7.93 (t, 1H), 7.8 (d/d, 3H), 7.5 (d, 1H), 7.46 (d, 2H), 4.09 (d, 1H), 3.76 (d, 1H), 3.67 (t, 1H), 3.6−3.2 (bm, 5H), 3.43 (s, 3H), 2.73 (s, 3H), 2.34 (m, 1H), 2.25 (quint., 2H),1.71/1.22 (dt, 2H). MS: m/z 481$[M + H]^+$.

5-[5-({3-[(1*R*,5*S*/1*S*,5*R*)-1-(4-Methoxyphenyl)-3-azabicyclo-[3.1.0]hex-3-yl]propyl}thio)-4-methyl-4H-1,2,4-triazol-3-yl]-2-methylquinoline Hydrochloride (18). The compound was obtained as a white, slightly hygroscopic, solid. ^{1}H NMR (1H, DMSO-d_6) δ: 10.57 (bs,1H), 8.28 (bs, 1H), 8.2 (d, 1H), 7.94 (t, 1H), 7.82 (d, 1H), 7.56 (d, 1H), 7.25 (d, 2H), 6.91 (d, 2H), 4.01 (dd, 1H), 3.7 (m, 1H), 3.74 (s, 3H), 3.6−3.2 (m, 6H), 3.42 (s, 3H), 2.75 (s, 3H), 2.24 (quint, 2H), 2.08 (quint, 1H), 1.62/1.05 (t/t, 2H). MS: m/z 486 $[M + H]^+$.

Derivative **18** was separated to give the separated enantiomers. Retention times given were obtained using an analytical supercritical fluid chromatography (Gilson) using a chiral column Chiralpak AD-H, 25 cm × 0.46 cm, eluent CO2 containing 20% (ethanol + 0.1% isopropyl alcohol), flow rate 2.5 mL/min, *P* 194 bar, *T* 35 °C, detection UV at 220 nm. Enantiomer **19** retention time = 39.2 min; enantiomer **20** retention time = 43.4 min.

5-[5-({3-[(1*S*,5*R*/1*R*,5*S*)-1-(4-Chlorophenyl)-3-azabicyclo[3.1.0]-hex-3-yl]propyl}thio)-4-methyl-4*H*-1,2,4-triazol-3-yl]-2-methylquinoline Hydrochloride (21). The compound was obtained as a white, slightly hygroscopic, solid. ^{1}H NMR (CD_3OD) δ: 8.95 (d,1H), 8.39 (d, 1H), 8.28 (t, 1H), 8.13 (d, 1H), 7.96 (d, 1H), 7.37 (m, 4H), 4.17 (d, 1H), 3.93 (d, 1H), 3.71 (m, 2H), 3.62 (s, 3H), 3.5 (2 m, 4H), 3.04 (s, 3H), 2.37 (m, 2H), 2.27 (m, 1H), 1.55 (m, 1H), 1.31 (m, 1H). MS: m/z 490 $[M + H]^+$.

Derivative **21** was separated to give the separated enantiomers. Retention times given were obtained using an analytical supercritical fluid chromatography (Berger) using a chiral column Chiralpak AD-H, 25 cm × 0.46 cm, eluent CO_2 containing 25% (ethanol + 0.1% isopropylamine), flow rate 2.5 mL/min, *P* 180 bar, *T* 35 °C, detection UV at 220 nm. Enantiomer **22**. Retention time = 24.3 min; enantiomer **23** retention time = 26.5 min.

2-Methyl-5-{4-methyl-5-[(3-{(1*S*,5*R*)-1-[4-(trifluoromethyl)-phenyl]-3-azabicyclo[3.1.0]hex-3-yl}propyl)thio]-4*H*-1,2,4-triazol-3-yl}quinoline Hydrochloride (24). MS: m/z 490 $[M + H]^+$. Retention time = 10.12 min (method A).

2-Methyl-6-{4-methyl-5-[(3-{(1*S*,5*R*)-1-[4-(trifluoromethyl)-phenyl]-3-azabicyclo[3.1.0]hex-3-yl}propyl)thio]-4*H*-1,2,4-triazol-3-yl}quinoline Hydrochloride (25). The compound was obtained as a white, slightly hygroscopic, solid. ^{1}H NMR (DMSO-d_6) δ: 10.41 (bs, HCl), 8.67 (bs, 1H), 8.47 (s, 1H), 8.2 (s, 2H), 7.72 (m, 1H), 7.68 (m, 2H), 7.49 (m, 2H), 4.07 (m, 1H), 3.74 (dd, 1H), 3.72 (s, 3H), 3.64 (dd, 1H), 3.51 (m, 1H), 3.3 (m, 4H), 2.81 (s, 3H), 2.28 (m, 1H), 2.19 (m, 2H), 1.72 (t, 1H), 1.19 (t, 1H). MS: m/z 524 $[M + H]^+$. Retention time = 10.17 min (method A).

(1*S*,5*R*)-3-{3-[(4-Methyl-5-phenyl-4*H*-1,2,4-triazol-3-yl)thio]-propyl}-1-[4-(trifluoromethyl)phenyl]-3-azabicyclo[3.1.0]hexane Hydrochloride (26). The compound was obtained as a white, slightly hygroscopic, solid. ^{1}H NMR (DMSO-d_6) δ: 10.3 (bs,), 7.7 (m, 4H), 7.57 (m, 4H), 7.49 (m, 1H), 4.11 (d, 1H), 3.76 (d, 1H), 3.66 (m, 1H), 3.61 (s, 3H), 3.52 (m, 1H), 3.30 (m, 4H), 2.29 (m, 1H), 2.17 (m, 2H), 1.63 (m, 1H), 1.22 (m, 1H). MS: m/z 459 $[M + H]^+$.

(1*S*,5*R*)-3-(3-{[4-Methyl-5-(2-methyl-3-pyridinyl)-4*H*-1,2,4-triazol-3-yl]thio}propyl)-1-[4-(trifluoromethyl)phenyl]-3-azabicyclo-[3.1.0]hexane Hydrochloride (27). The compound was obtained as a whitish, slightly hygroscopic, solid. ^{1}H NMR (DMSO-d_6) δ: 10.84 (bs, HCl), 8.77 (dd, 1H), 8.19 (bd, 1H), 7.71 (d, 2H), 7.66 (m, 1H), 7.51 (d, 2H), 4.08 (dd, 1H), ca. 3.8 (s, 3H), 3.8−3.3 (m, 7H), 2.54 (s, 3H), 2.30 (m, 1H), 2.22 (m, 2H), 1.83 (m, 1H), 1.20 (m, 1H). NMR (^{19}F, DMSO): δ −60.8. MS: m/z 474 $[M + H]^+$. Retention time = 9.35 min (method A).

(1*S*,5*R*)-3-(3-{[4-Methyl-5-(4-pyridazinyl)-4*H*-1,2,4-triazol-3-yl]-thio}propyl)-1-[4-(trifluoromethyl)phenyl]-3-azabicyclo[3.1.0]hexane Hydrochloride (28). The compound was obtained as a white, slightly hygroscopic, solid. ^{1}H NMR (DMSO-d_6) δ: 10.24 (bs, HCl), 9.56 (m, 1H), 9.39 (m, 1H), 8.01 (s, 1H), 7.64 (m, 2H), 7.44 (m, 2H), 4.08 (m, 1H), 3.68 (s, 3H), 3.58 (bm, 1H), 3.7−3.3 (m, 6H), 2.26 (m, 1H), 2.13 (m, 2H), 1.58 (t, 1H), 1.14 (t, 1H). MS: m/z 461 $[M + H]^+$. Retention time = 8.84 min (method A).

(1*S*,5*R*)-3-(3-{[4-Methyl-5-(5-pyrimidinyl)-4*H*-1,2,4-triazol-3-yl]-thio}propyl)-1-[4-(trifluoromethyl)phenyl]-3-azabicyclo[3.1.0]hexane Hhydrochloride (29). The compound was obtained as a off-white, slightly hygroscopic, solid. MS: m/z 461 $[M + H]^+$. Retention time = 8.92 min (method A).

(1*S*,5*R*)-3-(3-{[4-Methyl-5-(3-methyl-2-furanyl)-4*H*-1,2,4-triazol-3-yl]thio}propyl)-1-[4-(trifluoromethyl)phenyl]-3-azabicyclo-[3.1.0]hexane Hydrochloride (30). The compound was obtained as a white, slightly hygroscopic, solid. ^{1}H NMR (DMSO-d_6) δ: 10.56 (bs, HCl), 7.85 (d, 1H), 7.71 (d, 2H), 7.51 (d, 2H), 6.64 (d, 1H), 4.08 (dd, 1H), 3.75 (dd, 1H), 3.71 (s, 3H), 3.7−3.3 (m, 4H), 3.27 (t, 2H), 2.31 (m, 1H), 2.28 (s, 3H), 2.18 (m, 2H), 1.74 (t, 1H), 1.21 (t, 1H). MS: m/z 463 $[M + H]^+$. Retention time = 10.72 min (method A).

(1*S*,5*R*)-3-(3-{[4-Methyl-5-(6-methyl-3-pyridinyl)-4*H*-1,2,4-triazol-3-yl]thio}propyl)-1-[4-(trifluoromethyl)phenyl]-3-azabicyclo-[3.1.0]hexane Hydrochloride (31). The compound was obtained as a white, slightly hygroscopic, solid. MS: m/z 474 $[M + H]^+$. Retention time = 9.47 min (method A).

(1*S*,5*R*)-3-(3-{[5-(2,4-Dimethyl-1,3-thiazol-5-yl)-4-methyl-4*H*-1,2,4-triazol-3-yl]thio}propyl)-1-[4-(trifluoromethyl)phenyl]-3-azabicyclo[3.1.0]hexane Hhydrochloride (32). The compound was obtained as a white, slightly hygroscopic, solid. ^{1}H NMR (DMSO-d_6) δ: 10.61 (bs, 1H), 7.69 (d, 2H), 7.49 (d, 2H), 4.06 (d, 1H), 3.72 (t, 1H), 3.63 (d, 1H), 3.52 (t, 1H), 3.48 (s, 3H), 3.34 (t, 2H), 3.27 (t, 2H), 2.68 (s, 3H), 2.33 (m, 3H), 2.28 (m, 1H), 2.18 (m, 2H), 1.73 (t, 1H), 1.18 (t, 1H). MS: m/z 494 $[M + H]^+$. Retention time = 9.79 min (method A).

(1*S*,5*R*)-3-(3-{[4-Methyl-5-(5-methyl-2-pyrazinyl)-4*H*-1,2,4-triazol-3-yl]thio}propyl)-1-[4-(trifluoromethyl)phenyl]-3-azabicyclo-[3.1.0]hexane Hydrochloride (33). The compound was obtained as a white, slightly hygroscopic, solid. ^{1}H NMR (DMSO-d_6) δ: 10.41 (bs, HCl), 9.11 (bs, 1H), 8.63 (bs, 1H), 7.66 (d, 2H), 7.44 (d, 2H), 4.02 (dd, 1H), 3.83 (s, 3H), 3.68 (d, 1H), 3.6−3.2 (m, 6H), 2.54 (s, 3H), 2.25 (m, 1H), 2.14 (m, 2H), 1.65 (m, 1H), 1.14

(m, 1H). MS: m/z 475 $[M + H]^+$. Retention time = 10.15 min (method A).

(1*R*,5*S*/1*S*,5*R*)-3-(3-{[4-methyl-5-(4-methyl-1,3-oxazol-5-yl)-4*H*-1,2,4-triazol-3-yl]thio}propyl)-1-[4-(trifluoromethyl)phenyl]-3-azabicyclo[3.1.0]hexane Hydrochloride (34). The compound was obtained as a white, slightly hygroscopic, solid. ^{1}H NMR (DMSO-d_6) δ: 10.16 (bs, 1H), 8.58 (s, 1H), 7.72 (d, 2H), 7.51 (d, 2H), 4.1 (dd, 1H), 3.78 (dd, 1H), 3.70 (s, 3H), 3.66 (m, 2H), 3.29 (t, 2H), 2.5 (bm, 2H), 2.39 (s, 3H), 2.33 (quint, 2H), 2.19 (m, 1H), 1.62/1.23 (t/t, 2H). MS: m/z 464 $[M + H]^+$.

(1*S*,5*R*)-3-(3-{[4-Methyl-5-(4-methyl-1,3-oxazol-5-yl)-4*H*-1,2,4-triazol-3-yl]thio}propyl)-1-[4-(trifluoromethyl)phenyl]-3-azabicyclo[3.1.0]hexane Hydrochloride (35). The compound was obtained as a off white solid, slightly hygroscopic, solid. ^{1}H NMR (DMSO-d_6) δ: 10.16 (bs, 1H), 8.58 (s, 1H), 7.72 (d, 2H), 7.51 (d, 2H), 4.1 (dd, 1H), 3.78 (dd, 1H), 3.70 (s, 3H), 3.66 (m, 2H), 3.29 (t, 2H), 2.5 (bm, 2H), 2.39 (s, 3H), 2.33 (quint, 2H), 2.19 (m, 1H), 1.62/1.23 (t/t, 2H). MS: m/z 464 $[M + H]^+$.

(1*R*,5*S*)-3-(3-{[4-Methyl-5-(4-methyl-1,3-oxazol-5-yl)-4*H*-1,2,4-triazol-3-yl]thio}propyl)-1-[4-(trifluoromethyl)phenyl]-3-azabicyclo[3.1.0]hexane Hydrochloride (36). ^{1}H NMR (DMSO-d_6) δ: 10.16 (bs, 1H), 8.58 (s, 1H), 7.72 (d, 2H), 7.51 (d, 2H), 4.1 (dd, 1H), 3.78 (dd, 1H), 3.70 (s, 3H), 3.66 (m, 2H), 3.29 (t, 2H), 2.5 (bm, 2H), 2.39 (s, 3H), 2.33 (quint, 2H), 2.19 (m, 1H), 1.62/1.23 (t/t, 2H). MS: m/z 464 $[M + H]^+$.

(1*R*,5*S*/1*S*,5*R*)-3-(3-{[4-Methyl-5-(4-methyl-1,3-oxazol-5-yl)-4H-1,2,4-triazol-3-yl]thio}propyl)-1-phenyl-3-azabicyclo[3.1.0]-hexane Hydrochloride (37). The compound was obtained as a white, slightly hygroscopic, solid. ^{1}H NMR (DMSO-d_6) δ: 10.46 (bs,1H), 8.58 (s, 1H), 7.4−7.2 (m, 5H), 4.04 (dd, 1H), 3.73 (m, 1H), 3.7 (s, 3H), 3.7−3.4 (m, 2H), 3.4−3.2 (m + t, 4H), 2.39 (s, 3H), 2.17 (m, 3H), 1.64,1.1 (2t, 2H). MS: m/z 396 $[M + H]^+$.

(1*R*,5*S*/1*S*,5*R*)-1-(4-*tert*-Butylphenyl)-3-(3-{[4-methyl-5-(4-methyl-1,3-oxazol-5-yl)-4*H*-1,2,4-triazol-3-yl]thio}propyl)-3-azabicyclo[3.1.0]hexane Hydrochloride (38). The compound was obtained as a white, slightly hygroscopic, solid. ^{1}H NMR (CD_3OD) δ: 8.4 (s, 1H), 7.42 (d, 2H), 7.28 (d, 2H), 4.11 (d, 1H), 3.88 (d, 1H), 3.8 (s, 3H), 3.65 (m, 2H), 3.43 (t, 2H), 3.39 (t, 2H), 2.47 (s, 3H), 2.29 (m, 2H), 2.21 (m, 1H), 1.44 (m, 1H), 1.33 (s, 9H), 1.3 (m, 1H). MS: m/z 452 $[M + H]^+$.

(1*R*,5*S*)-1-(4-*tert*-Butylphenyl)-3-(3-{[4-methyl-5-(4-methyl-1,3-oxazol-5-yl)-4*H*-1,2,4-triazol-3-yl]thio}propyl)-3-azabicyclo-[3.1.0]hexane Hydrochloride (39). The compound was obtained as a white, slightly hygroscopic, solid. ^{1}H NMR (CD_3OD) δ: 8.4 (s, 1H), 7.42 (d, 2H), 7.28 (d, 2H), 4.11 (d, 1H), 3.88 (d, 1H), 3.8 (s, 3H), 3.65 (m, 2H), 3.43 (t, 2H), 3.39 (t, 2H), 2.47 (s, 3H), 2.29 (m, 2H), 2.21 (m, 1H), 1.44 (m, 1H), 1.33 (s, 9H), 1.3 (m, 1H). MS: m/z 452 $[M + H]^+$.

(1*S*,5*R*)-1-(4-*tert*-Butylphenyl)-3-(3-{[4-methyl-5-(4-methyl-1,3-oxazol-5-yl)-4*H*-1,2,4-triazol-3-yl]thio}propyl)-3-azabicyclo-[3.1.0]hexane Hydrochloride (40). The compound was obtained as a white, slightly hygroscopic, solid. ^{1}H NMR (CD_3OD) δ: 8.4 (s, 1H), 7.42 (d, 2H), 7.28 (d, 2H), 4.11 (d, 1H), 3.88 (d, 1H), 3.8 (s, 3H), 3.65 (m, 2H), 3.43 (t, 2H), 3.39 (t, 2H), 2.47 (s, 3H), 2.29 (m, 2H), 2.21 (m, 1H), 1.44 (m, 1H), 1.33 (s, 9H), 1.3 (m, 1H). MS: m/z 452 $[M + H]^+$.

(1*R*,5*S*/1*S*,5*R*)-1-(4-Bromophenyl)-3-(3-{[4-methyl-5-(4-methyl-1,3-oxazol-5-yl)-4*H*-1,2,4-triazol-3-yl]thio}propyl)-3-azabicyclo-[3.1.0]hexane Hydrochloride (41). The compound was obtained as a white, slightly hygroscopic, solid. ^{1}H NMR (DMSO-d_6) δ: 10.29 (bs,1H), 8.58 (s, 1H), 7.55 (dd, 2H), 7.27 (dd, 2H), 4.03 (dd, 1H), 3.73 (dd, 1H), 3.7 (s, 3H), 3.55 (m, 2H), 3.5−3.2/3.28 (m + t, 4H), 2.39 (s, 3H), 2.19 (m, 3H), 1.59/1.12 (2t, 2H). MS: m/z 474 $[M + H]^+$.

Compound **41** was separated to give the separated enantiomers. Retention times given were obtained using an analytical supercritical fluid chromatography (Gilson) using a chiral column Chiralpak AS-H, 25 cm × 0.46 cm, eluent CO2 containing 10% (ethanol + 0.1% isopropyilamine), flow rate 2.5 mL/min, *P* 199 bar, *T* 35 °C, detection UV at 220 nm. Enantiomer **42** retention time = 22.2 min. Specific optical rotation of the corresponding free base: [α]D = −51° ($CHCl_3$, *T* = 20 °C, *c* = 0.00913 g/mL); enantiomer 43 retention time = 30.8 min. Specific optical rotation of the corresponding free base: enantiomer 2, specific optical rotation of the corresponding free base [α]D = +27° ($CHCl_3$, *T* = 20 °C, *c* = 0.0113 g/mL).

(1*R*,5*S*/1*S*,5*R*)-1-(4-Methoxyphenyl)-3-(3-{[4-methyl-5-(4-methyl-1,3-oxazol-5-yl)-4*H*-1,2,4-triazol-3-yl]thio}propyl)-3-azabicyclo-[3.1.0]hexane Hydrochloride (44). The title compound was obtained as a white slightly hygroscopic solid. ^{1}H NMR (DMSO-d_6) δ: 10.18 (bs, 1H), 8.58 (s, 1H), 7.24 (d, 2H), 6.91 (d, 2H), 3.97 (dd, 1H), 3.74 (s, 3H), 3.7 (s, 3H), 3.7 (m, 1H), 3.6−3.2 (m, 4H), 3.27 (t, 2H), 2.39 (s, 3H), 2.15 (quint, 2H), 2.07 (quint, 1H), 1.49/1.05 (2t, 2H). MS: m/z 426 $[M + H]^+$.

Compound **44** was separated to give the separated enantiomers. Retention times given were obtained using an analytical supercritical fluid chromatography (Gilson) using a chiral column Chiralpak AS-H, 25 cm × 0.46 cm, eluent CO2 containing 8% (ethanol + 0.1% isopropylamine), flow rate 2.5 mL/min, *P* 190 bar, *T* 35 °C, detection UV at 220 nm. Enantiomer **45** retention time = 28.7 min; enantiomer **46** retention time = 36.4 min.

(1*S*,5*R*/1*R*,5*S*)-3-(3-{[4-Methyl-5-(4-methyl-1,3-oxazol-5-yl)-4*H*-1,2,4-triazol-3-yl]thio}propyl)-1-[3-(methyloxy)phenyl]-3-azabicyclo[3.1.0]hexane Hydrochloride (47). The title compound was obtained as a white, slightly hygroscopic solid. ^{1}H NMR (DMSO-d_6) δ: 10.16 (bs,1H), 8.58 (d, 1H), 7.26 (dd, 1H), 6.85 (m, 3H), 4.03 (dd, 1H), 3.77 (s, 3H), 3.72 (dd, 1H), 3.7 (s, 3H), 3.6−3.3 (bm, 4H), 3.28 (t/m, 2H), 2.39 (s, 3H), 2.18 (m, 3H), 1.53−1.1 (t/m, 2H). MS: m/z 426 $[M + H]^+$.

Compound **47** was separated to give the separated enantiomers. Retention times given were obtained using an analytical supercritical fluid chromatography (Berger) using a chiral column Chiralcel OJ-H, 25 cm × 0.46 cm, eluent CO_2 containing 13% (2-propanol + 0.1% isopropylamine), flow rate 2.5 mL/min, *P* 180 bar, *T* 35 °C, detection UV at 220 nm. Enantiomer **48** retention time = 24.2 min; enantiomer **49** retention time = 26.8 min.

(1*S*,5*R*/1*R*,5*S*)-1-(4-Chlorophenyl)-3-(3-{[4-methyl-5-(4-methyl-1,3-oxazol-5-yl)-4*H*-1,2,4-triazol-3-yl]thio}propyl)-3-azabicyclo-[3.1.0]hexane Hydrochloride (50). The title compound was obtained as a white, slightly hygroscopic solid. ^{1}H NMR (DMSO-d_6) δ: δ 9.93(bs,1H), 8.58 (s, 1H), 7.42 (d, 2H), 7.33 (d, 2H), 4.04 (dd, 1H), 3.75 (dd, 1H), 3.7 (s, 3H), 3.5 (m, 2H), 3.3 (bm, 4H), 2.39 (s, 3H), 2.2 (m, 1H), 2.15 (m, 2H), 1.47−1.14 (2t, 2H). MS: m/z 431 $[M + H]^+$.

Compound **50** was separated to give the separated enantiomers. Retention times given were obtained using an analytical supercritical fluid chromatography (Gilson) using a chiral column Chiralpak AS-H, 25 cm × 0.46 cm, eluent CO_2 containing 15% (ethanol + 0.1% isopropylamine), flow rate 2.5 mL/min, *P* 190 bar, *T* 35 °C, detection UV at 220 nm. Enantiomer **51** retention time = 7.8 min. Specific optical rotation of the corresponding free base: [α]D = −25° ($CHCl_3$, *T* = 20 °C, *c* = 0.0066 g/mL). Enantiomer **52** retention time = 9.7 min. Specific optical rotation of the corresponding free base: [α]D = +29° ($CHCl_3$, *T* = 20 °C, *c* = 0.0068 g/mL)

(1*S*,5*R*/1*R*,5*S*)-1-(3-Chlorophenyl)-5-methyl-3-(3-{[4-methyl-5-(4-methyl-1,3-oxazol-5-yl)-4*H*-1,2,4-triazol-3-yl]thio}propyl)-3-azabicyclo[3.1.0]hexane Hydrochloride (53). The title compound was obtained as a white slightly hygroscopic solid. ^{1}H NMR (DMSO-d_6) δ: 9.88 (bs,1H), 8.58 (s, 1H), 7.43 (d, 1H), 7.4−7.2 (m, 3H), 4.06 (dd, 1H), 3.75 (dd, 1H), 3.7 (s, 3H), 3.62−3.54 (t/m, 2H), 3.5−3.3 (bm, 4H), 2.39 (s, 3H), 2.25 (m, 1H), 2.15 (m, 2H), 1.46−1.19 (2 m, 2H). MS: m/z 431 $[M + H]^+$.

Compound **53** was separated to give the separated enantiomers. Retention times given were obtained using an analytical supercritical fluid chromatography (Berger) using a chiral column Chiralpak AD-H, 25 cm × 0.46 cm, eluent CO_2 containing 15% (ethanol + 0.1% isopropylamine), flow rate 2.5 mL/min, *P* 180 bar, *T* 35 °C, detection UV at 220 nm. Enantiomer **54** retention time = 29.6 min; enantiomer **55** retention time = 32.0 min.

(1*S*,5*R*/1*R*,5*S*)-1-(4-Fluorophenyl)-3-(3-{[4-methyl-5-(4-methyl-1,3-oxazol-5-yl)-4*H*-1,2,4-triazol-3-yl]thio}propyl)-3-azabicyclo-[3.1.0]hexane Hydrochloride (56). The title compound was obtained as a white slightly hygroscopic solid. ^{1}H NMR (DMSO-d_6) δ: 10.06 (bs,1H), 8.58 (s, 1H), 7.36 (dd, 2H), 7.19 (t, 2H), 4.02 (dd, 1H), 3.74 (dd, 1H), 3.7 (s, 3H), 3.55 (m, 2H), 3.5−3.2 (bm, 4H), 2.39 (s, 3H), 2.15 (m, 3H), 1.49−1.1 (2t, 2H). MS: *m*/*z* 414 $[M + H]^+$.

Compound **56** was separated to give the separated. Retention times given were obtained using an analytical supercritical fluid chromatography (Gilson) using a chiral column Chiralpak AS-H, 25 cm × 0.46 cm, eluent CO_2 containing 6% (ethanol + 0.1% isopropylamine), flow rate 2.5 mL/min, *P* 190 bar, *T* 35 °C, detection UV at 220 nm. Enantiomer **57** retention time = 26.2 min; enantiomer **58** retention time = 32.4 min

(1*S*,5*R*/1*R*,5*S*)-1-(3-Fluorophenyl)-3-(3-{[4-methyl-5-(4-methyl-1,3-oxazol-5-yl)-4*H*-1,2,4-triazol-3-yl]thio}propyl)-3-azabicyclo-[3.1.0]hexane Hydrochloride (59). The title compound was obtained as a white slightly hygroscopic solid. ^{1}H NMR (DMSO-d_6) δ: 10.21 (bs,1H), 8.58 (d, 1H), 7.4 (m, 1H), 7.2−7.0 (m, 3H), 4.03 (dd, 1H), 3.75 (dd, 1H), 3.7 (s, 3H), 3.61 (t/m, 1H), 3.52 (m, 1H), 3.3 (m, 2H), 3.28 (t, 2H), 2.38 (s, 3H), 2.25 (m, 1H), 2.16 (m, 2H), 1.57−1.17 (t/m, 2H). MS: *m*/*z* 414 $[M + H]^+$.

Compound **59** was separated to give the separated. Retention times given were obtained using an analytical supercritical fluid chromatography (Gilson) using a chiral column Chiralpak AS-H, 25 cm × 0.46 cm, eluent CO_2 containing 6% (ethanol + 0.1% isopropylamine), flow rate 2.5 mL/min, *P* 190 bar, *T* 35 °C, detection UV at 220 nm. Enantiomer **60** retention time = 24.6 min; enantiomer **61** retention time = 26.0 min

(1*R*,5*S*/1*S*,5*R*)-3-(3-{[4-Methyl-5-(4-methyl-1,3-oxazol-5-yl)-4*H*-1,2,4-triazol-3-yl]thio}propyl)-1-[3-(trifluoromethyl)phenyl]-3-azabicyclo[3.1.0]hexane Hydrochloride (62). The title compound was obtained as a white slightly hygroscopic solid. ^{1}H NMR (DMSO-d_6) δ: 10.5 (bs,1H), 8.58 (s, 1H), 7.7−7.5 (m, 4H), 4.09 (m, 1H), 3.8−3.2 (m, 8H), 3.29 (t, 2H), 2.39 (s, 3H), 2.3 (m, 1H), 2.18 (m, 2H), 1.68 (t, 1H), 1.21 (t, 1H). MS: *m*/*z* 464 $[M + H]^+$.

Compound **62** was separated to give the separated. Retention times given were obtained using an analytical supercritical fluid chromatography (Gilson) using a chiral column Chiralpak AD-H, 25 cm × 0.46 cm, eluent CO_2 containing 10% (ethanol + 0.1% 2-propanol), flow rate 22 mL/min, *P* 190 bar, *T* 36 °C, detection UV at 220 nm. Enantiomer **63** retention time = 17.6 min; enantiomer **64** retention time = 18.4 min

(1*R*,5*S*/1*S*,5*R*)-3-(3-{[4-Methyl-5-(4-methyl-1,3-oxazol-5-yl)-4*H*-1,2,4-triazol-3-yl]thio}propyl)-1-[2-(trifluoromethyl)phenyl]-3-azabicyclo[3.1.0]hexane Hydrochloride (65). The title compound was obtained as a white slightly hygroscopic solid. ^{1}H NMR (DMSO-d_6) δ: 10.48 (bs,1H), 8.55 (s, 1H), 7.9−7.6 (m, 4H), 3.9−3.1 (bm, 8H), 3.68 (s, 3H), 2.36 (s, 3H), 2.13 (m, 2H), 1.66 (m, 1H), 1.2 (m, 1H), 1.1 (m, 1H). MS: *m*/*z* 464 $[M + H]^+$.

(1*S*,5*R*/1*R*,5*S*)-3-(3-{[4-Methyl-5-(4-methyl-1,3-oxazol-5-yl)-4*H*-1,2,4-triazol-3-yl]thio}propyl)-1-{4-[(trifluoromethyl)oxy]-phenyl}-3-azabicyclo[3.1.0]hexane Hydrochloride (66). The title compound was obtained as a white slightly hygroscopic solid. ^{1}H NMR (DMSO-d_6) δ: 10.33 (bs,1H), 8.58 (s, 1H), 7.43 (d, 2H), 7.36 (d, 2H), 4.04 (dd, 1H), 3.73 (dd, 1H), 3.7 (s, 3H), 3.6−3.2 (bm, 6H), 2.39 (s, 3H), 2.2 (m, 3H), 1.61−1.16 (2t, 2H). MS: *m*/*z* 480 $[M + H]^+$.

Compound **66** was separated to give the separated enantiomers. Retention times given were obtained using chiral column Chiracel OD, 25 cm × 0.46 cm, eluent A: *n*-hexane; B: 2-propanol, gradient isocratic 10% B v/v, flow rate 1 mL/min, detection UV at 220 nm. Enantiomer **67** retention time = 28.3 min; enantiomer **68** retention time = 50.6 min.

(1*R*,5*S*/1*S*,5*R*)-1-(3,4-Dichlorophenyl)-3-(3-{[4-methyl-5-(4-methyl-1,3-oxazol-5-yl)-4*H*-1,2,4-triazol-3-yl]thio}propyl)-3-azabicyclo[3.1.0]hexane Hydrochloride (69). The title compound was obtained as a white slightly hygroscopic solid. ^{1}H NMR (DMSO-d_6) δ: 10.11 (vbs, 1H), 8.58 (s, 1H), 7.6 (d + d, 2H), 6.29 (dd, 1H), 4.04/3.74 (2dd, 2H), 3.7 (s, 3H), 3.6−3.2 (m, 4H), 3.28 (t, 2H), 2.39 (s, 3H), 2.26 (quint, 1H), 2.15 (quint, 2H), 1.53/1.2 (2t, 2H). MS: *m*/*z* 464 $[M + H]^+$.

Compound **69** was separated to give the separated enantiomers. Retention times given were obtained using an analytical supercritical fluid chromatography (Gilson) using a chiral column Chiralpak AS-H, 25 cm × 0.46 cm, eluent CO_2 containing 8% (ethanol + 0.1% isopropylamine), flow rate 2.5 mL/min, *P* 190 bar, *T* 35 °C, detection UV at 220 nm. Enantiomer **70** retention time = 38.0 min; enantiomer **71** retention time = 40.8 min.

(1*R*,5*S*/1*S*,5*R*)-1-[2-Fluoro-4-(trifluoromethyl)phenyl]-3-(3-{[4-methyl-5-(4-methyl-1,3-oxazol-5-yl)-4*H*-1,2,4-triazol-3-yl]thio}-propyl)-3-azabicyclo[3.1.0]hexane Hydrochloride (72). The title compound was obtained as a white slightly hygroscopic solid. ^{1}H NMR (DMSO-d_6) δ: 10.28 (bs,1H), 8.58 (s, 1H), 7.73 (d, 1H), 7.6 (m, 2H), 4/ 3.57 (d/m, 2H), 3.79 (d, 1H), 3.69 (s, 3H), 3.5−3.2 (vbm, 1H), 3.27 (t, 2H), 2.5 (m, 2H), 2.4 (m, 1H), 2.38 (s, 3H), 2.14 (quint, 2H), 1.62/1.16 (2t, 2H). MS: *m*/*z* 481 $[M + H]^+$.

Compound **72** was separated to give the separated. Retention times given were obtained using an analytical HPLC using a chiral column Chiralpak AD-H 5 μm, 250 mm × 4.6 mm, eluent A, *n*-hexane; B, 2-propanol, gradient isocratic 15% B, flow rate 0.8 mL/min, detection UV at 200−400 nm. Enantiomer **73** retention time = 15.4 min; enantiomer **74** retention time = 16.3 min.

(1*S*,5*R*/1*R*,5*S*)-3-(3-{[4-Methyl-5-(4-methyl-1,3-oxazol-5-yl)-4*H*-1,2,4-triazol-3-yl]thio}propyl)-1-[2-methyl-4-(trifluoromethyl)-phenyl]-3-azabicyclo[3.1.0]hexane Hydrochloride (75). The title compound was obtained as a white slightly hygroscopic solid. ^{1}H NMR (DMSO-d_6) δ: 10.25 (bs,1H), 8.58 (s, 1H), 7.6 (m, 3H), 3.97−3.7 (dd/m, 2H), 3.79/3.4 (dd/m, 2H), 3.69 (s, 3H), 3.27 (t, 2H), 2.5 (m, 2H), 2.48 (s, 3H), 2.38 (s, 3H), 2.2 (m, 1H), 2.13 (quint, 2H), 1.61−1.01 (2t, 2H). MS: *m*/*z* 478 $[M + H]^+$.

(1*R*,5*S*/1*S*,5*R*)-1-[4-Fluoro-3-(trifluoromethyl)phenyl]-3-(3-{[4-methyl-5-(4-methyl-1,3-oxazol-5-yl)-4*H*-1,2,4-triazol-3-yl]thio}-propyl)-3-azabicyclo[3.1.0]hexane Hydrochloride (76). The title compound was obtained as a white slightly hygroscopic solid. ^{1}H NMR (DMSO-d_6) δ: 10.2 (bs, 1H), 8.58 (s, 1H), 7.75 (dm, 1H), 7.72 (m, 1H), 7.53 (t, 1H), 4.06 (dd, 1H), 3.74 (dd, 1H), 3.7 (s, 3H), 3.6 (m, 2H), 3.4 (m, 2H), 3.28 (t, 2H), 2.39 (s, 3H), 2.26 (m, 1H), 2.18 (m, 2H), 1.54 (t, 1H), 1.22 (dd, 1H). MS: *m*/*z* 481 $[M + H]^+$.

Compound **76** was separated to give the separated. Retention times given were obtained using an analytical supercritical fluid chromatography (Gilson) using a chiral column Chiralpak AS-H, 25 cm × 0.46 cm, eluent CO_2 containing 8% (ethanol + 0.1% isopropylamine), flow rate 2.5 mL/min, *P* 180 bar, *T* 35 °C, detection UV at 220 nm. Enantiomer **77** retention time = 25.9 min; enantiomer **78** retention time = 28.3 min.

(1*R*,5*S*/1*S*,5*R*)-1-[2-Fluoro-5-(trifluoromethyl)phenyl]-3-(3-{[4-methyl-5-(4-methyl-1,3-oxazol-5-yl)-4*H*-1,2,4-triazol-3-yl]thio}-propyl)-3-azabicyclo[3.1.0]hexane Hydrochloride (79). The title compound was obtained as a white slightly hygroscopic solid. ^{1}H NMR (CD_3OD) δ: 8.41 (s,1H), 7.8 (m, 1H), 7.74 (m, 1H), 7.39 (t, 1H), 4.13 (d, 1H), 3.95 (d, 1H), 3.81 (s, 3H), 3.73 (bd, 1H), 3.54 (d, 1H), 3.48 (m, 2H), 3.41 (m, 2H), 2.48 (s, 3H), 2.39 (m, 1H), 2.28 (q, 2H), 1.58 (m, 1H), 1.35 (m, 1H). MS: *m*/*z* 482 $[M + H]^+$.

Compound **79** was separated to give the separated. Retention times given were obtained using an analytical supercritical fluid chromatography (Berger) using a chiral column Chiralpak AD-H, 25 cm × 0.46 cm, eluent CO_2 containing 7% (ethanol + 0.1% isopropylamine), flow rate 2.5 mL/min, *P* 180 bar, *T* 35 °C, detection UV at 220 nm. Enantiomer **80** retention time = 21.2 min; enantiomer **81** retention time = 22.7 min.

(1*R*,5*S*/1*S*,5*R*)-1-[2-Fluoro-3-(trifluoromethyl)phenyl]-3-(3-{[4-methyl-5-(4-methyl-1,3-oxazol-5-yl)-4*H*-1,2,4-triazol-3-yl]thio}-propyl)-azabicyclo[3.1.0]hexane Hydrochloride (82). The title compound was obtained as a white slightly hygroscopic solid. ^{1}H NMR (CD_3OD) δ: 8.46 (s,1H), 7.75−7.65 (m, 2H), 7.38 (t,

1H), 4.1 (d, 1H), 3.93 (d, 1H), 3.78 (s, 3H), 3.71 (d, 1H), 3.54 (d, 1H), 3.48 (t, 2H), 3.38 (t, 2H), 2.45 (s, 3H), 2.36 (m, 1H), 2.25 (m, 2H), 1.54 (m, 1H), 1.34 (m, 1H). MS: m/z 481 $[M + H]^+$.

Compound **82** was separated to give the separated. Retention times given were obtained using an analytical supercritical fluid chromatography (Gilson) using a chiral column Chiralpak AD-H, 250 mm × 4.6 mm, eluent *n*-hexane/ethanol 88/12 (isocratic), flow rate 1 mL/min, *P* 200−400 bar, *T* 36 °C, detection UV at 200−400 nm. Enantiomer **83** retention time = 20.4 min; enantiomer **84** retention time = 23.0 min.

(1*R*,5*S*/1*S*,5*R*)-1-[3-Fluoro-4-(trifluoromethyl)phenyl]-5-methyl-3-(3-{[4-methyl-5-(4-methyl-1,3-oxazol-5-yl)-4*H*-1,2,4-triazol-3-yl]-thio}propyl)-3-azabicyclo[3.1.0]hexane Hydrochloride (85). The title compound was obtained as a white slightly hygroscopic solid. ^{1}H NMR (CD_3OD) δ: 8.4 (s, 1H), 7.55 (t, 1H), 7.37 (d, 1H), 7.32 (d, 1H), 4.2 (d, 1H), 3.91 (d, 1H), 3.81 (s, 3H), 3.76 (d, 1H), 3.67 (d, 1H), 3.51 (t, 2H), 3.43 (t, 2H), 2.47 (s, 3H), 2.41 (m, 1H), 2.31 (m, 2H), 1.61 (t, 1H), 1.45 (t, 1H). MS: m/z 496 $[M + H]^+$.

Compound **85** was separated to give the separated. Retention times given were obtained using an analytical supercritical fluid chromatography (Berger) using a chiral column Chiralpak AD-H, 25 cm × 0.46 cm, eluent CO_2 containing 10% (ethanol + 0.1% isopropylamine), flow rate 2.5 mL/min, *P* 180 bar, *T* 35 °C, detection UV at 220 nm. Enantiomer **86** retention time = 27.1 min; enantiomer **87** retention time = 31.0 min.

(1*R*,5*S*/1*S*,5*R*)-1-[3-Fluoro-5-(trifluoromethyl)phenyl]-3-(3-{[4-methyl-5-(4-methyl-1,3-oxazol-5-yl)-4*H*-1,2,4-triazol-3-yl]thio}-propyl)-azabicyclo[3.1.0]hexane Hydrochloride (88). The title compound was obtained as a white slightly hygroscopic solid. ^{1}H NMR (CD_3OD) δ: 8.46 (s,1H), 7.54 (bs, 1H), 7.47 (bd, 1H), 7.41 (bd, 1H), 4.19 (d, 1H), 3.09 (d, 1H), 3.87 (s, 3H), 3.71 (m, 2H), 3.51 (t, 2H), 3.46 (t, 2H), 2.49 (s, 3H), 2.33 (m, 3H), 1.67 (m, 1H), 1.39 (m, 1H). MS: m/z 482 $[M + H]^+$.

Compound **88** was separated to give the separated enantiomers. Retention times given were obtained using an analytical supercritical fluid chromatography (Gilson) using a chiral column Chiralpak AD-H, 25 cm × 0.46 cm, eluent CO_2 containing 10% (ethanol + 0.1% isopropyilamine), flow rate 2.5 mL/min, *P* 180 bar, *T* 35 °C, detection UV at 220 nm. Enantiomer **89** retention time = 12.6 min; enantiomer **90** retention time = 14.7 min.

(1*R*,5*S*/1*S*,5*R*)-1-(2-Fluoro-4-methylphenyl)-3-(3-{[4-methyl-5-(4-methyl-1,3-oxazol-5-yl)-4*H*-1,2,4-triazol-3-yl]thio}propyl)-3-azabicyclo[3.1.0]hexane Hydrochloride (91). The title compound was obtained as a white slightly hygroscopic solid. ^{1}H NMR (CD_3OD) δ: 8.39 (s, 1H), 7.26 (t, 1H), 7.01 (m, 2H), 3.93 (m,1H), 3.77 (m, 4H), 3.61 (m, 1H), 3.41−3.38 (m, 5H), 2.47 (s, 3H), 2.36 (s, 3H), 2.23 (m, 2H), 2.19 (m, 1H), 1.45 (t, 1H), 1.21 (t, 1H). MS: m/z 428 $[M + H]^+$.

Compound **91** was separated to give the separated enantiomers. Retention times given were obtained using an analytical supercritical fluid chromatography (Berger) using a chiral column Chiralpak AD-H, 25 cm × 0.46 cm, eluent CO_2 containing 25% (ethanol + 0.1% isopropyilamine), flow rate 2.5 mL/min, *P* 180 bar, *T* 35 °C, detection UV at 220 nm. Enantiomer **92** retention time = 13.7 min; enantiomer **93** retention time = 16.2 min.

(1*R*,5*S*/1*S*,5*R*)-1-[4-(4-Chloro-2-fluorophenyl]-3-(3-{[4-methyl-5-(4-methyl-1,3-oxazol-5-yl)-4*H*-1,2,4-triazol-3-yl]thio}propyl)-azabicyclo[3.1.0]hexane Hydrochloride (94). The title compound was obtained as a white slightly hygroscopic solid. ^{1}H NMR (CD_3OD) δ: 8.27 (s, 1H), 7.3 (t, 1H), 7.1 (m, 2H), 3.95 (d, 1H), 3.8 (d, 1H), 3.67 (s, 3H), 3.56 (dd, 1H), 3.4−3.2 (m, 5H), 2.34 (s, 3H), 2.15 (m, 3H), 1.4 (t, 1H), 1.18 (t, 1H). MS: m/z 448 $[M + H]^+$.

Compound **94** was separated to give the separated enantiomers. Retention times given were obtained using an analytical HPLC using a chiral column Chiralpak AD-H 5 μm, 250 mm × 21 mm; eluent A, *n*-hexane; B, ethanol + 0.1% isopropylamine, gradient isocratic 20% B, flow rate 6 mL/min, detection UV at 225 nm. Enantiomer **95** retention time = 18.7 min; enantiomer **96** retention time = 20.6 min.

(1R,5*S*/1*S*,5*R*)-1-[4-(Methyloxy)-5-(trifluoromethyl)phenyl]-3-(3-{[4-methyl-5-(4-methyl-1,3-oxazol-5-yl)-4*H*-1,2,4-triazol-3-yl]-thio}propyl)-azabicyclo[3.1.0]hexane Hydrochloride (97). The title compound was obtained as a white slightly hygroscopic solid. ^{1}H NMR (CD_3OD) δ: 8.37 (s,1H), 7.57 (m, 2H), 7.17 (d, 1H) 3.9 (m, 4H), 3.77 (s, 3H), 3.74 (m, 1H), 3.65−3.30 (m, 6H), 2.44 (s, 3H), 2.21 (m, 2H), 2.13 (m, 1H), 1.43 (t, 1H), 1.24 (m, 1H). MS: m/z 494 $[M + H]^+$.

Compound **97** was separated to give the separated. Retention times given were obtained using an analytical supercritical fluid chromatography (Gilson) using a chiral column Chiralpak AD-H, 250 mm × 4.6 mm, eluent *n*-hexane/ethanol 70/30 (isocratic), flow rate 0.8 mL/min, detection UV at 200−400 nm. Enantiomer **98** retention time = 15.5 min; enantiomer **99** retention time = 17.5 min.

(1*R*,5*S*/1*S*,5*R*)-1-[3-Chloro-4-(methyloxy)phenyl]-3-(2-{[4-methyl-5-(4-methyl-1,3-oxazol-5-yl)-4*H*-1,2,4-triazol-3-yl]thio}propyl)-3-azabicyclo[3.1.0]hexane Hydrochloride (100). The title compound was obtained as a white slightly hygroscopic solid. ^{1}H NMR (CD_3OD) δ: 8.4 (s,1H), 7.35 (m, 1H), 7.1 (m, 2H), 4.01 (m,1H), 3.89 (m,4H), 3.8 (s, 3H), 3.6−3.3 (m, 6H), 2.47 (s, 3H), 2.23 (m, 2H), 2.19 (m, 1H), 1.4 (m, 1H), 1.2 (m, 1H). MS: m/z 460 $[M + H]^+$.

Compound **100** was separated to give the separated enantiomers. Retention times given were obtained using an analytical supercritical fluid chromatography (Berger) using a chiral column Chiralpak AD-H, 25 cm × 0.46 cm, eluent CO_2 containing 25% (ethanol + 0.1% isopropyilamine), flow rate 2.5 mL/min, *P* 180 bar, *T* 35 °C, detection UV at 220 nm. Enantiomer **101** retention time = 13.7 min; enantiomer **102** retention time = 16.2 min.

(1*R*,5*S*/1*S*,5*R*)-1-[3-(2-{[4-Methyl-5-(4-methyl-1,3-oxazol-5-yl)-4*H*-1,2,4-triazol-3-yl]thio}propyl)-1-{3-[(trifluoromethyl)oxy]-phenyl}-3-azabicyclo[3.1.0]hexane Hydrochloride (103). The title compound was obtained as a white slightly hygroscopic solid. ^{1}H NMR (CD_3OD) δ: 8.41 (s, 1H), 7.49 (t, 1H), 7.3 (s, 1H), 7.37 (d, 1H), 7.24 (m,1H), 4.17 (d,1H), 3.9 (d, 1H), 3.8 (s, 3H), 3.69 (d, 2H), 3.51 (t, 2H), 3.42 (t, 2H), 2.47 (s, 3H), 2.3 (m, 3H), 1.57 (dd, 1H), 1.36 (t, 1H). MS: m/z 480 $[M + H]^+$.

Compound **103** was separated to give the separated enantiomers. Retention times given were obtained using an analytical supercritical fluid chromatography (Berger) using a chiral column Chiralpak AD-H, 25 cm × 0.46 cm, eluent CO_2 containing 12% (ethanol + 0.1% isopropyilamine), flow rate 2.5 mL/min, *P* 180 bar, *T* 35 °C, detection UV at 220 nm. Enantiomer **104** retention time = 10.7 min; enantiomer **105** retention time = 12.0 min.

Computational Modeling. Construction of the hERG Models. The closed state of the hERG channel was modeled based on its homology with the bacterial Kcsa structure from *Streptococcus lividans*, solved in 1998 by McKinnon et al.[24] Alignment of the pore region and the S6 helix is obvious from the key GYG motif (GFG in hERG) and the key hinge glycine in S6. The alignment of the S5 helices of hERG and Kcsa, however, was not obvious. This was based finally on the observation of a highly conserved glutamate at the extracellular side of S5, which is found in most potassium channels. An NMR structure of the S5-SS1 loop peptide has been published,[25] which suggests that this region is largely helical. This was added to the model as a helix-turn-β-strand motif. The tetrameric ensemble was fully minimized using the CHARMm program,[26] with an initial 500 steps of Steepest Descent, followed by 5000 steps of ABNR, and a constant dielectric of 5. Helical H-bonding distance constraints were used to maintain the overall fold of the bundle.

An open state model was also built using the rat Kv1.2 structure as a template.[27] The same S5 glutamate, pore GYG, and S6 glycine residues were used to generate the alignment. Use was made of the S5-SS1 loop model constructed for the closed state structure and the same CHARMm conditions were used for final refinement.

Construction of the Dopamine D_3 Receptor Models. The model of the dopamine D_3 receptor was built using our "in house"

program GPCR_Builder.[28] This is an automated 7TM receptor homology modeling program which incorporates a database of all known human and rodent Family A receptor sequences and a prealigned set of transmembrane domains for these. The models are based on the TM domain taken from the crystal structure of bovine rhodopsin.[29] A special set of optimized 3D templates are used to add the extracellular loops. An internal rotamer library is then applied to all residue side chains except those conserved residues known to be involved in an important functional role (e.g., the asparagines in TM1 and TM7, the aspartate on TM2, and the DRY motif on TM3). The program automatically generates a CHARMm script, which can be used for model optimization and ligand docking. Typically, the same set of conditions as those described for the hERG models above were used during the minimization stage. A strict alignment between rhodopsin and dopamine D_3 gives rise to a very short loop length (2 residues) between the disulfide bonded cysteine in the second extracellular loop and the top of TM5. During the optimization some unfolding of the extracellular side of TM5 is therefore allowed by relaxing the helical distance constraints in this region. This is in keeping with the reported SCAM results carried out by Javitch et al. on the D_2 receptor.[30]

Automated Docking of Ligands in the Receptor and Channel Models. Partial atomic charges fitted to the electrostatic potential derived from semiempirical wave functions (MNDO) were calculated with MOPAC.[31] All calculations were performed in vacuum.

Automatic docking experiments were performed with Monte Carlo sampling followed by energy minimization (MCEM) using MacroModel routines and AMBER* force field. Subsequently poses were ranked according to their interaction energy defined as the difference between the energy of the complex ($E_{complex}$) and the energy of the ligand (E_{ligand}) and that of the protein ($E_{protein}$):

$$E_{\text{interaction energy}} = E_{\text{complex}} - E_{\text{ligand}} - E_{\text{protein}}$$

Poses were visually inspected within Maestro and evaluated for their consistency with with SAR data generated within the same structural class.

Acknowledgment. We thank all the colleagues who helped in generating the data reported in this manuscript, Drs. Caterina Mazzoni, Chiara Savoia, and Maria Pilla, and Enzo Valerio. We also thank in particular Drs. Anne Andorn and Barbara Bertani for the fruitful discussion during the preparation of this manuscript.

References

(1) Heidbreder, C. A.; Gardner, E. L.; Xi, Z-X; Thanos, P. K.; Mugnaini, M.; Hagan, J. J.; Ashby, C. R., Jr. The role of central DA D_3 receptors in drug addiction: a review of pharmacological evidence. *Brain Res. Rev.* **2005**, *49*, 77–105.

(2) Joyce, J. N.; Millan, M. J. DA D3 receptor antagonists as therapeutic agents. *Drug Discovery Today* **2005**, *10*, 917–925.

(3) Micheli, F.; Heidbreder, C. Selective DA D3 receptor antagonists: A review 2001−2005. *Recent Pat. CNS Drug Discovery* **2006**, *1*, 271–288.

(4) Newman, A. H.; Grundt, P.; Nader, M. A. DA D3 receptor partial agonists and antagonists as potential drug abuse therapeutic agents. *J. Med. Chem.* **2005**, *48*, 3663–3679.

(5) Micheli, F.; Heidbreder, C. A. Selective Dopamine D3 Receptor Antagonists; 1997−2007: A Decade of Progress. *Expert Opin. Ther. Pat.* **2008**, *18*, 821–840.

(6) Heidbreder, C. Selective antagonism at dopamine D3 receptors as a target for drug addiction pharmacotherapy: a review of preclinical evidence. *CNS Neurol. Disord. Drug Targets* **2008**, *7*, 410–421.

(7) Micheli, F.; Bonanomi, G.; Blaney, F. E.; Braggio, S.; Capelli, A. M.; Checchia, A.; Curcuruto, O.; Damiani, F.; Di-Fabio, R.; Donati, D.; Gentile, G.; Gribble, A.; Hamprecht, D.; Tedesco, G.; Terreni, S.; Tarsi, L.; Lightfoot, A.; Pecoraro, M.; Petrone, M.; Perini, O.; Piner, J.; Rossi, T.; Worby, A.; Pilla, M.; Valerio, E.; Griffante, C.; Mugnaini, M.; Wood, M.; Scott, C.; Andreoli, M.; Lacroix, L.; Schwarz, A.; Gozzi, A.; Bifone, A.; Ashby, C. R., Jr.; Hagan, J. J.; Heidbreder, C. 1,2,4-Triazol-3-yl-thiopropyl-tetrahydrobenzazepines: a series of potent and selective dopamine D3 receptor antagonists. *J. Med. Chem.* **2007**, *50*, 5076–5089.

(8) Micheli, F.; Bonanomi, G.; Braggio, S.; Capelli, A. M.; Celestini, P.; Damiani, F.; Di Fabio, R.; Donati, D.; Gagliardi, S.; Gentile, G.; Hamprecht, D.; Petrone, M.; Radaelli, S.; Tedesco, G.; Terreni, S.; Worby, A.; Heidbreder, C. New fused benzazepine as selective D_3 receptor antagonists. Synthesis and biological evaluation. Part one: [h]-fused tricyclic systems. *Bioorg. Med. Chem. Lett.* **2008**, *18*, 901–907.

(9) Micheli, F.; Bonanomi, G.; Braggio, S.; Capelli, A. M.; Celestini, P.; Damiani, F.; Di Fabio, R.; Donati, D.; Gagliardi, S.; Gentile, G.; Hamprecht, D.; Perini, O.; Petrone, M.; Radaelli, S.; Tedesco, G.; Terreni, S.; Worby, A.; Heidbreder, C. New fused benzazepine as selective D_3 receptor antagonists. Synthesis and biological evaluation. Part two: [g]-fused and hetero fused systems. *Bioorg. Med. Chem. Lett.* **2008**, *18*, 908–912.

(10) Bonanomi, G.; Checchia, A.; Fazzolari, E.; Hamprecht, D.; Micheli, F.; Tarsi, L.; Terreni, S. 3-(1,2,4-Triazol-3-ylalkyl) azabiciclo [3.1.0] hexane derivatives as modulators of dopamine D3 receptors. Patent WO 2006108701, **2006**.

(11) Arista, L.; Cardullo, F.; Checchia, A.; Hamprecht, D.; Micheli, F.; Tedesco, G.; Terreni, S.. Preparation of 3-azabicyclo[3.1.0]hexanes as selective modulators of dopamine D3 receptors. Patent WO 2006133946, **2006**.

(12) The research complied with national legislation and with company policy on the Care and Use of Animals and with related codes of practice.

(13) Atkinson, F.; Bravi, G. *The SAR Toolkit*, UK-QSAR and Chemo-Informatics Group Meeting, October 2007; Abstract (http://www.iainm.demon.co.uk/ukqsar/meetings/2007-10-11.html#abstract_e013-ca26c3a3c590184b907a3d2668c2) and presentation (http://www.documentarea.com/qsar/Francis_Atkinson07.pdf.

(14) *Daylight v4.92*; Chemical Information Systems Inc.: Aliso Viejo, CA, http://www.daylight.com.

(15) *Spotfire Decision Site 8.2.1*; available from http://www.spotfire.com/.

(16) Aptuit Limited, 3 Simpson Parkway, Livingston,West Lothian, EH54 7BH, Scotland, www.aptuit.uk.

(17) Mitcheson, J. S.; Chen, J.; Lin, M.; Culberson, C.; Sanguinetti, M. C. A structural basis for drug-induced long QT syndrome. *Proc. Natl. Acad. Sci.U.S.A.* **2000**, *97*, 12329–12333.

(18) Sanguinetti, M. C.; Mitcheson, J. S. Predicting drug-hERG channel interactions that cause acquired long QT syndrome. *Trends Pharmacol. Sci.* **2005**, *26*, 119–124.

(19) CERB, Chemin de Montifault, 18800 Baugy, France www.cerb.fr.

(20) Burris, K. D.; Filtz, T. M.; Chumpradit, S.; Kung, M. P.; Foulon, C; Hensler, J. G.; Kung, H. F.; Molinoff, P. B. Characterization of [^{125}I](*R*)-*trans*-7-hydroxy-2-[*N*-propyl-*N*-(3′-iodo-2′-propenyl)amino] tetralin binding to dopamine D_3 receptors in rat olfactory tubercle. *J. Pharmacol. Exp. Ther.* **1994**, *268*, 935–942.

(21) Dewey, S. L.; Brodie, J. D.; Gerasimov, M; Horan, B; Gardner, E. L.; Ashby, C. R., Jr. A pharmacologic strategy for the treatment of nicotine addiction. *Synapse* **1999**, *31*, 76–86.

(22) Horan, B; Smith, M; Gardner, E. L.; Lepore, M; Ashby, C. R., Jr. (−)-Nicotine produces conditioned place preference in Lewis, but not Fischer 344 rats. *Synapse* **1997**, *26*, 93–94.

(23) Horan, B; Gardner, E. L.; Dewey, S. L.; Brodie, J. D.; Ashby, C. R., Jr. The selective sigma(1) receptor agonist, 1-(3,4-dimethoxyphenethyl)-4-(phenylpropyl)piperazine (SA4503), blocks the acquisition of the conditioned place preference response to (−)-nicotine in rats. *Eur. J. Pharmacol.* **2001**, *426*, R1–R2.

(24) Kaab, S.; Dixon, J.; Duc, J.; Ashen, D.; Nabauer, M.; Beuckelmann, D. J.; Steinbeck, G.; McKinnon, D.; Tomaselli, G. F. Molecular basis of transient outward potassium current downregulation in human heart failure: a decrease in Kv4.3 mRNA correlates with a reduction in current density. *Circulation* **1998**, *98*, 1383–1393.

(25) Torres, A. M.; Bansal, P. S.; Sunde, M.; Clarke, C. E.; Bursill, J. A.; Smith, D. J.; Bauskin, A.; Breit, S. N.; Campbell, T. J.; Alewood, P. F.; Kuchel, P. W.; Vandenberg, J. I. Structure of the HERG K^+ Channel S5P Extracellular Linker: Role of an Amphipathic alpha-Helix in C-Type Inactivation. *J. Biol. Chem.* **2003**, *278*, 42136–42148.

(26) www.accelrys.com.

(27) Magis, C.; Gasparini, D.; Lecoq, A.; Le Du, M. H.; Stura, E.; Charbonnier, J. B.; Mourier, G.; Boulain, J.-C.; Pardo, L.; Caruana, A.; Joly, A.; Lefranc, M.; Masella, M.; Menez, A.; Cuniasse, P. Structure-Based Secondary Structure-Independent Approach To Design Protein Ligands: Application to the Design of Kv1..2 Potassium Channel Blockers. *J. Am. Chem. Soc.* **2006**, *128*, 16190–16205.

(28) Blaney, F. E.; Tennant, M. (1996) Computational tools and results in the construction of G protein-coupled receptor models. In *Membrane Protein Models*; Findlay J. B. C., Ed.; Bios Scientific Publishers Ltd.: Oxford, 1996; pp 161−176.
(29) Polczewski, K.; Kumasaka, T.; Hori, T.; Behnke, C. A.; Motoshima, H.; Fox, B. A.; Le Trong, I.; Teller, D. C.; Okada, T.; Stenkamp, R. E.; Yamamoto, M. Miyano, M. Crystal structure of rhodopsin: a G protein-coupled receptor. *Science* **2000**, *289*, 739−745.
(30) Shi, L.; Simpson, M. M.; Ballesteros, J. A.; Javitch, J. A.. The First Transmembrane Segment of the Dopamine D2 Receptor: Accessibility in the Binding-Site Crevice and Position in the Transmembrane Bundle. *Biochemistry* **2001**, *40*, 12339–12348.
(31) www.openmopac.com.